Molecular Therapy
Nucleic Acids
Original Article

miRNA-642a-3p protects β cells from glucolipotoxicity

Sandra Sofia Pinhanços,[1,2,8,18] João Teixeira de Oliveira,[3,4] C. Henrique Alves,[5,6,7,8] Cláudia M. Deus,[17] Twan J.J. de Winter,[9,10] Sofia Viana,[5,7,8,11,12,19] Flávio Reis,[5,7,8,11] Jorge Santos,[3,4] Mijke Buitinga,[13,14] Françoise Carlotti,[9] Lino Ferreira,[1,8,16] Martin Gotthardt,[15] John Jones,[1,8] and Hugo Fernandes[1,2,8,16,17]

[1]CNC - Center for Neuroscience and Cell Biology, University of Coimbra, 3060-197 Coimbra, Portugal; [2]IIIUC-Institute of Interdisciplinary Research, University of Coimbra, 3004-517 Coimbra, Portugal; [3]UMIB (Unidade Multidisciplinar de Investigação Biomédica) ICBAS-UP, 4050-346 Porto, Portugal; [4]Centro Hospitalar Universitário do Porto (CHUPORTO), 4050-342 Porto, Portugal; [5]Clinical Academic Center of Coimbra (CACC), 3004-561 Coimbra, Portugal; [6]Association for Innovation and Biomedical Research on Light and Image (AIBILI), 3000-548 Coimbra, Portugal; [7]University Coimbra, Coimbra Institute for Clinical and Biomedical Research (iCBR), Faculty of Medicine, 3000-548 Coimbra, Portugal; [8]University Coimbra, Center for Innovative Biomedicine and Biotechnology (CIBB), 3004-531 Coimbra, Portugal; [9]Department of Internal Medicine, Leiden University Medical Center, 2333 ZA Leiden, the Netherlands; [10]Department of Anatomy and Embryology, Leiden University Medical Center, 2333 ZA Leiden, the Netherlands; [11]Institute of Pharmacology & Experimental Therapeutics & Coimbra Institute for Clinical and Biomedical Research (iCBR), Faculty of Medicine, University of Coimbra, 3000-075 Coimbra, Portugal; [12]Polytechnic Institute of Coimbra, ESTESC - Coimbra Health School, 3046-854 Coimbra, Portugal; [13]Nutrition and Movement Sciences, Maastricht University, 6211 LK Maastricht, the Netherlands; [14]Radiology and Nuclear Medicine, Maastricht UMC, 6200 MD Maastricht, the Netherlands; [15]Department of Medical Imaging, Radboud University Medical Centre, 6525 GA Nijmegen, the Netherlands; [16]Faculty of Medicine, University of Coimbra, 3000-548 Coimbra, Portugal; [17]MIA-Portugal, University of Coimbra, 3004-504 Coimbra, Portugal; [18]University of Coimbra, Institute for Interdisciplinary Research, Doctoral Programme in Experimental Biology and Biomedicine (PDBEB), 3030-789 Coimbra, Portugal; [19]H&TRC - Health and Technology Research Center, Coimbra Health School, Polytechnic University of Coimbra, Coimbra, Portugal

The incidence of type 2 diabetes mellitus (T2DM) is tightly linked to obesity. High levels of circulating glucose and saturated free fatty acids (FFAs), known as glucolipotoxicity (GLT), is implicated in β cell dysfunction and/or death. This study aims to identify miRNAs capable of protecting β cells from GLT-induced cell death (GICD). A library of 2,080 human miRNA mimics was transfected in β cells followed by exposure to GLT. We identified 45 miRNAs capable of protecting β cells from GICD and selected miR-642a-3p for further studies. RNA-seq revealed that miR-642a-3p restored the expression of β cell identity genes and modulated pathways associated with cell survival and lipid metabolism. Moreover, we showed that transfection of β cells with miR-642a-3p protected them from GLT-induced changes in insulin secretion. Compared with the control, hypercaloric-fed mice showed a trend toward decreased expression of GLT-protective miRNAs. Notably, we demonstrated that miR-642a-3p expression was downregulated in human islets isolated from T2DM patients compared with non-diabetic controls. Importantly, in obese patients, the expression of GLT-protective miRNAs in plasma-derived extracellular vesicles was increased in non-diabetic patients. Overall, we have identified a potential dual role for miR-642a-3p as both a biomarker and a facilitator of β cell survival and function, offering a novel theranostic tool for the management of diabetes and/or obesity.

INTRODUCTION

Type 2 diabetes mellitus (T2DM) is a chronic, progressive, and multifactorial disease characterized by uncontrolled elevated glucose levels secondary to β cell dysfunction and/or death.[1,2]

Obesity is a critical risk factor for the development of T2DM[3] and it is associated with elevated concentrations of circulating free fatty acids (FFAs).[4] Increased plasma concentrations of saturated FFAs, such as palmitate (PA), negatively affect β cell function and may constitute a key link between obesity and diabetes.[5] *In vitro* exposure of β cells to high concentrations of FFAs and glucose recapitulates glucolipotoxicity (GLT)—a pathophysiological condition found *in vivo* in pancreatic islets of obese patients and a well-established model to study the mechanisms governing β cell dysfunction and/or death.[6,7] GLT impinges on β cell health and function[8] via several different mechanisms including oxidative stress and mitochondrial dysfunction,[4] lipid droplet (LD) formation,[9] modulation of survival pathways such as AKT and FOXO1 signaling,[10] loss of β cell identity genes,[11] and impairment of β cell glucose-stimulated insulin secretion (GSIS).[11]

However, the risk of developing diabetes is not uniform among individuals with obesity, suggesting the existence of protective mechanisms. In this context, studies have shown that microRNAs (miRNAs) may provide protection against T2DM, even in the presence of obesity.[12] Several miRNAs are known to regulate glucose and lipid metabolism.[13] For instance, miR-34a[14,15] and miR-21[16] were involved in β cell apoptosis, miR-375 was associated with insulin synthesis and secretion,[17] and miR-17-3p was involved in the proliferation and

Received 23 February 2024; accepted 28 February 2025;
https://doi.org/10.1016/j.omtn.2025.102498.

Correspondence: Hugo Fernandes, CNC - Center for Neuroscience and Cell Biology, University of Coimbra, 3060-197 Coimbra, Portugal.
E-mail: hugo.fernandes@uc.pt

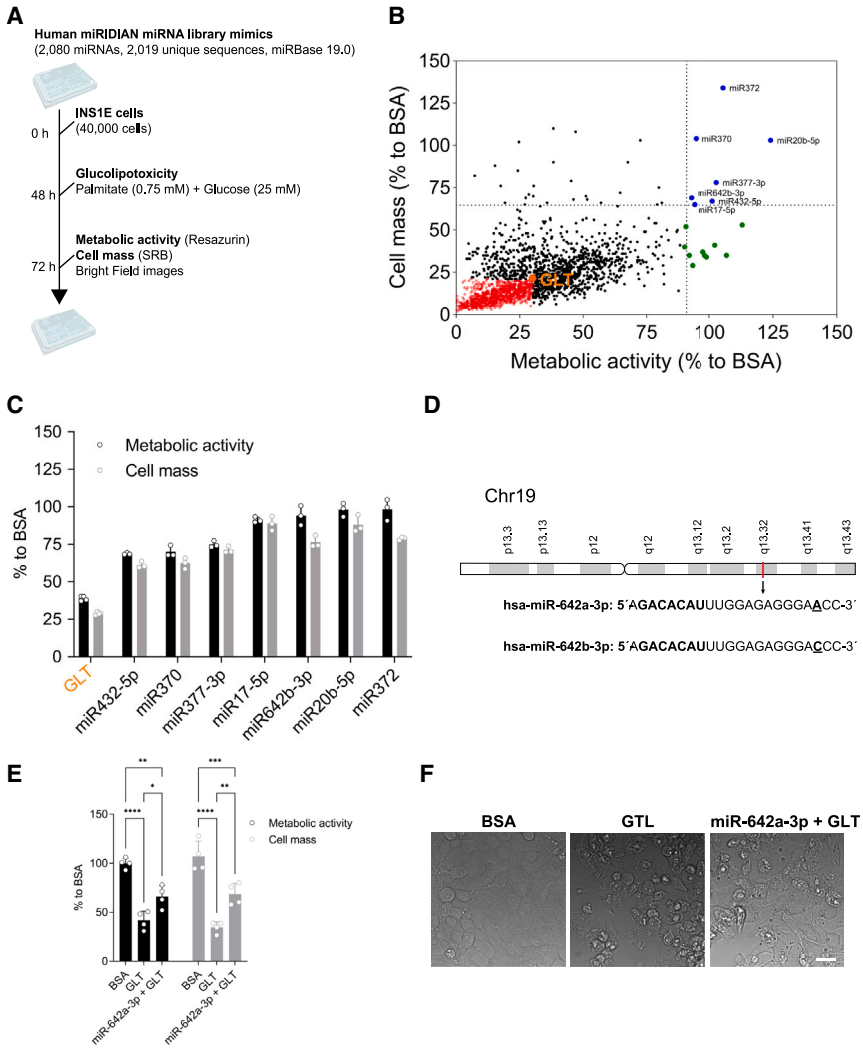

Figure 1. High-throughput screening assay to identify miRNAs capable of protecting β cells from GLT

(A) Schematic overview of the screening workflow used in the HTS. (B) Metabolic activity versus cell mass (% to BSA) for each individual miRNA tested in the primary screening. miRNAs capable of increasing the metabolic activity are colored (the ones that increase both the cell mass as well as the metabolic activity are highlighted in blue). (C) Validation of the seven miRNAs identified in the primary screening as capable of increasing both the metabolic activity as well as the cell mass. The results were normalized to BSA-containing medium condition ($n = 3$ independent experiments). (D) miR-642 location on chromosome 19 and mature sequence for miR-642a-3p and miR-642b-3p, respectively. Bold, seed sequence; underlined, different nucleotide between miR-642a-3p and miR-642b-3p. (E and F) Metabolic activity and cell mass (% to BSA control) and bright-field images, respectively, of INS1E cells transfected with miR-642a-3p and exposed to GLT conditions for 24 h. Statistical analysis was performed by two-way ANOVA, followed by Tukey's multiple comparisons test. ****$p < 0.001$. Results are presented as mean ± SD ($n = 4$ biological replicates, each biological replicate containing three technical replicates). Scale bar, 50 μm.

survival of β cells.[18] Moreover, overexpression of miR-190 exerted protective effects against glucotoxicity-induced β cell damage by attenuating the over-production of ROS and alleviating oxidative stress.[19] Since one miRNA can regulate the expression of multiple mRNAs, they play a key role in governing gene networks where multiple genes interact to orchestrate cellular responses. Consequently, miRNA-based therapies present an innovative and promising approach for addressing complex diseases such as diabetes and obesity.[20]

Bariatric surgery (BS) remains a prominent and highly effective strategy for addressing obesity and T2DM, and a significant number of patients achieve remission in a relatively short period.[21] Although the precise mechanisms are not fully elucidated, ongoing studies are actively exploring whether miRNAs may contribute to the observed therapeutic effects.[22]

In this study, we set out to identify miRNAs capable of protecting β cells from GLT-induced β cell death (GICD) followed by validation of those miRNAs in *in vitro* and *in vivo* models (mouse and human).

RESULTS

Identification of miRNAs capable of protecting β cells from GICD

INS1E cells, insulin-producing β cells known to be susceptible to PA-induced apoptosis[23] were selected for the high-throughput screening (HTS) assay. INS1E cells were exposed to increasing concentrations of PA for 24 h in medium containing 1% (v/v) fetal bovine serum (FBS) and either 11 or 25 mM glucose. Metabolic activity and cell mass were quantified as indirect measurements of metabolism, viability, and proliferation, respectively.[24,25] The GLT condition selected for the HTS assay (0.75 mM PA and 25 mM glucose in medium with 1% [v/v] FBS) induced a 62% and a 71% decrease in metabolic activity and cell mass, respectively (Figure S1). A library containing 2,080 human miRNA mimics was screened (Figure 1A). A non-targeting miRNA (miR-SRC) and a Lipofectamine (LP) control were included in the HTS assay (Figure S2). miRNAs capable of increasing the metabolic activity and/or cell mass more than 3 times the mean of the GLT condition were considered a hit. On this basis, we identified 45 hits: 17 miRNAs increased the metabolic activity and 28 the cell mass (Figure 1B; Table S1). Notably, 7 miRNAs (miR-432-5p, miR-370, miR-377-3p, miR-17-5p, miR-642b-3p, miR-372, and miR-20a-5p) increased both metabolic activity and cell mass (blue dots, Figure 1B). Using the same experimental conditions of the primary screening and three technical replicates, we

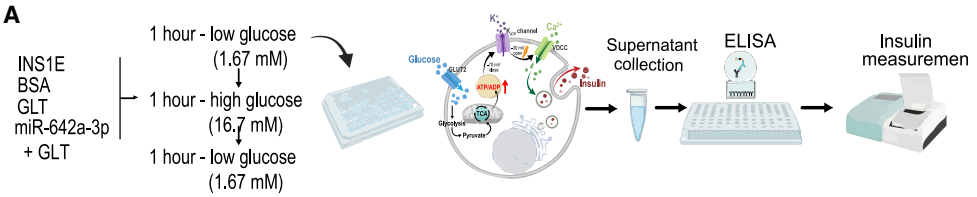

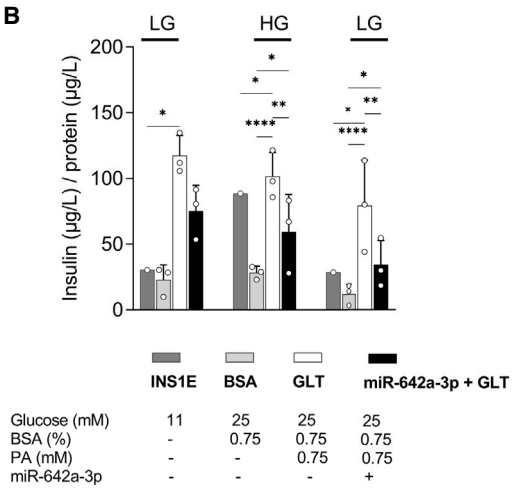

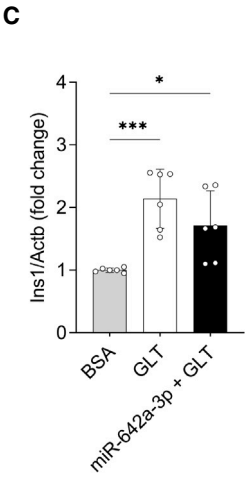

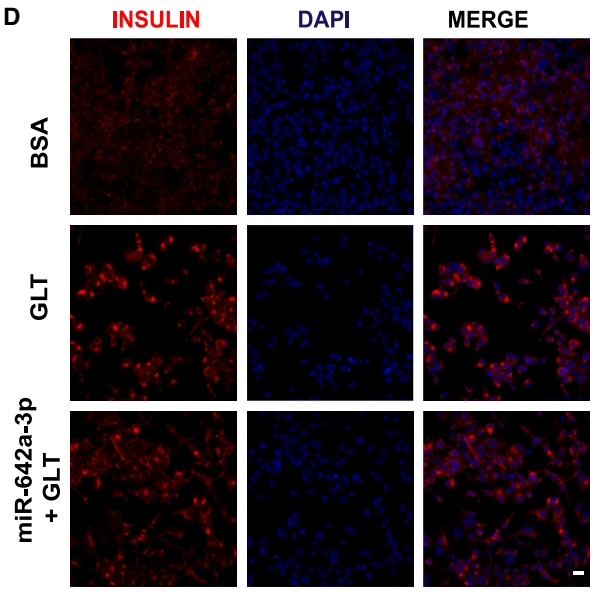

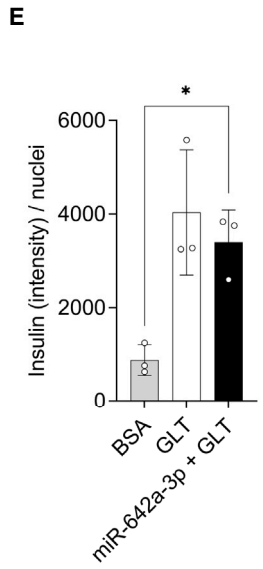

(legend on next page)

confirmed that these 7 miRNAs were able to protect β cells from GICD (Figure 1C; Table S2).

miR-642a-3p protects β cells from GICD and loss of function

One of the hits, miR-642b-3p, belongs to the same family as miR-642a-3p, a miRNA recently identified by us as capable of enhancing the survival of endothelial cells (ECs) exposed to ischemia-mimicking conditions.[26] These two miRNAs differ by one single nucleotide and, more importantly, share the same seed sequence (Figure 1D).

Given the potential impact of a single miRNA on two phenotypes highly relevant to diabetes (protection against GLT and survival of ECs), we selected miR-642a-3p for mechanistic studies. Firstly, we confirmed that miR-642a-3p effectively protected β cells from GICD resulting in a 1.57-fold increase in metabolic activity and 1.97-fold increase in cell mass, compared with GLT condition (Figures 1E and 1F). Next, we determined the impact of GLT and miR-642a-3p in β cell function. Our results showed that β cells increased insulin secretion in response to glucose stimulation, reverting to baseline levels upon exposure to low glucose concentration. Strikingly, compared with the control, exposure of β cells to GLT led to a significant increase in insulin secretion, regardless of the glucose concentration. Notably, transfection of β cells with miR-642a-3p protected β cells from the changes elicited by GLT (Figures 2A and 2B). These results were further confirmed using immunofluorescence and qRT-PCR (Figures 2C–2E).

miR-642a-3p opposes GLT-induced transcriptional changes in β cells

RNA-seq analysis showed that, compared with the control, exposure of β cells to GLT resulted in a total of 4,666 DEG (4,221 upregulated and 445 downregulated). Volcano plots and hierarchical clustering were generated to compare gene expression between GLT- and bovine serum albumin (BSA)-treated β cells (Figures 3A and 3B; Table S3). Our results showed that genes upregulated by GLT were associated with positive regulation of apoptotic processes, intrinsic apoptotic signaling pathways in response to endoplasmic reticulum stress, cytokine-cytokine receptor interaction, MAPK signaling pathway, and apoptosis, whereas downregulated genes were associated with cell division, chromosome segregation, mitotic cytokinesis, and cell cycle and homologous recombination (Figures 3C and 3D). Overall, these results suggest that GLT treatment downregulates cell division pathways and upregulates those involved in inflammation and apoptosis.

Compared with GLT-treated β cells, transfection with miR-642a-3p followed by GLT exposure resulted in a total of 5,039 DEG (2,969 upregulated and 2,070 downregulated). Volcano plots and hierarchical clustering were generated to compare gene expression between miR-642a-3p and GLT-treated β cells (Figures 3E and 3F; Table S4). Our results showed that genes upregulated by miR-642a-3p were associated with chromatin remodeling, cell migration, mitotic cytokinesis and axon guidance, focal adhesion, MAPK signaling pathway, and the PI3K-Akt signaling pathway, whereas downregulated genes were associated with the intrinsic apoptotic signaling pathway in response to endoplasmic reticulum stress, negative regulation of fat cell differentiation, positive regulation of apoptotic process and dopaminergic synapse, relaxin signaling pathway, and insulin signaling pathway (Figures 3G and 3H).

Given the fact that the putative targets of miR-642a-3p should be found among the downregulated genes, we transfected β cells with miR-642a-3p for 48 h and, compared with the control, our results showed a total of 7,495 DEG (3,538 up and 3,921 down). Using the filtering criteria described in the methods, functional annotation and gene ontology (GO) enrichment analysis revealed that the upregulated genes were involved in synapse organization, neuron differentiation, and regulation of inflammatory responses, whereas the downregulated genes were involved in synapse assembly and miRNA loading onto RISC (Figure S3; Tables S5 and S6). From the list of downregulated genes, and after applying the filtering criteria, we ended up with 238 genes. To narrow our search, we intersected this list with the list of putative targets retrieved from TargetScan and miRWalk, resulting in a final list of 72 genes (set A) (Table S7). Finally, this list of 72 putative targets was intersected with the list of genes downregulated upon transfection of β cells with miR-642a-3p followed by exposure to GLT (115 genes) (set B) (Table S8), resulting in 7 common genes: *Wdr13*, *Zdhhc7*, *Prkab2*, *Cmtm6*, *Akt2*, *Dusp4*, and *Dnajc27* (Figure 3I). To validate these targets, we performed an independent experiment and used RT-PCR to analyze the expression of the selected genes. Compared with the control, our results showed that exposure of β cells to GLT did not affect the expression of *Wdr13*, *Prkab2*, *Akt2*, and *Dnajc27* but inhibited the expression of *Zdhhc7*. However, upon transfection of β cells with miR-642a-3p, our results showed a statistically significant inhibition in the expression of *Wdr13*, *Zdhhc7*, *Dusp4*, and *Dnajc27* and a trend toward decreased expression of *Cmtm6* and *Akt2* (Figure 3J). Finally, to further validate that the inhibition of these genes could phenocopy the protective effects observed with miR-642a-3p, we individually knockdown *Wdr13*, *Zdhhc7*, *Dusp4*, *Dnajc27*, and *Cmtm6* using short-interference RNAs (siRNAs) under conditions similar to those reported for the primary screening and subsequent validation assays. Our results showed that only the inhibition of *Cmtm6* was able to recapitulate the protective effect observed with miR-642a-3p (Figure 3K). *In silico* prediction pairing between the hsa-miR-642a-3p

Figure 2. Effect of miR-642a-3p in β cell function

(A) Schematic overview of glucose-stimulated insulin secretion (GSIS) assay in INS1E cells. (B) Quantification of insulin secretion evaluated by ELISA. (C and D) Representative images of immunofluorescence staining for insulin in INS1E cells exposed to control, GLT, and miR-642a-3p and their respective quantification. (E) RT-PCR analysis of insulin expression in INS1E cells exposed to GLT or miR-642a-3p and GLT. The results are the average of three independent experiments. Statistics was determined using two-way ANOVA followed by Tukey's multiple comparison test. $^{*}p < 0.0388$, $^{**}p < 0.0051$, $^{***}p = 0.0007$, $^{****}p < 0.0001$. Error bars represent SD. Scale bar, 25 μm.

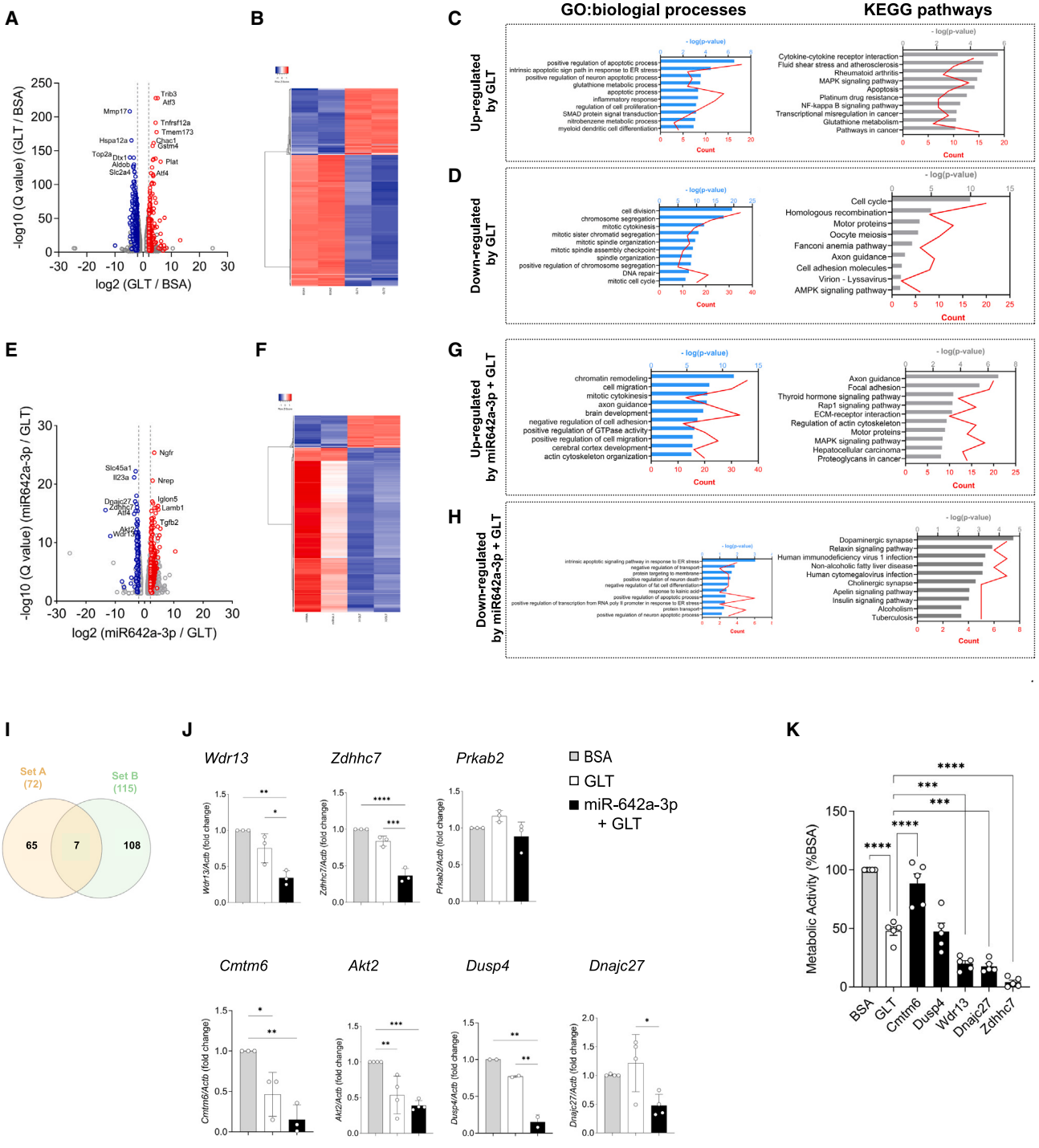

Figure 3. RNA-seq for INS1E cells exposed to GLT and miR-642a-3p

(A) Volcano plot for INS1E cells treated with BSA and GLT showing the magnitude of the gene expression changes (log2 fold-change; x axis) and statistical differences (–log10 q value; y axis). (B) Heatmaps highlighting the differential expression of genes between BSA vs. GLT (412 downregulated and 210 upregulated). (C) Gene ontology analysis (biological processes [BP] and KEGG pathways) for genes upregulated by GLT. (D) GO:BP and KEGG pathways for genes downregulated by GLT. (E) Volcano plot GLT vs. miR-642a-3p showing the magnitude of the gene expression change (log2 fold-change; x axis) and statistical differences (–log10 q value; y axis). (F) Heat maps between

(legend continued on next page)

and the 3′ UTR of rat Cmtm6 mRNA is shown in Figure S4. Overall, these findings suggest that *Cmtm6* could be one of the targets of miR-642a-3p.

miR-642a-3p restores the expression of β cell identity markers after exposure to GLT and activates pro-survival signaling pathways

We analyzed the impact of GLT and miR-642a-3p in the expression of genes related to β cell identity (*Foxa2*, *Nkx6.1*, *Mafa*, and *Pdx1*) (Figures 4A–4D). Our RNA-seq results indicated that exposure of β cells to GLT downregulated the expression of *Foxa2* and that miR-642a-3p restored its expression. However, in an independent experiment and using RT-PCR analysis, we showed no differences in the expression of *Foxa2* (Figure 4A). Next, we showed that, compared with the control, exposure of β cells to GLT significantly downregulated the expression of *Nkx6.1* and *Mafa*, whereas transfection with miR-642a-3p was sufficient to maintain the expression of these genes (Figures 4B and 4C). Moreover, compared with the BSA control and the GLT condition, miR-642a-3p significantly upregulated the expression of *Pdx1* (Figure 4D). Interestingly, inhibition of *Cmtm6* followed by exposure to GLT also resulted in the upregulation of the β cell identity gene *Pdx1*, but not *Nkx6.1*, *Foxa2*, and *Mafa* (Figure S5B). We further extended this evaluation to genes involved in lipid metabolism (fatty acid synthase [*Fasn*]), oxidative stress (catalase [*Cat*] and thioredoxin-binding protein [*Txnip*]), and β cell function (Paired Box 6 [*Pax6*]) (Figure S6). RNA-seq analysis revealed that exposure of β cells to GLT resulted in the downregulation of *Fasn*, *Txnip*, and *Pax6* genes. Remarkably, transfection with miR-642a-3p increased the expression of *Fasn*, *Cat*, and *Pax6* compared with the GLT condition. By RT-PCR analysis, and compared with the control, we demonstrated a statistically significant downregulation of *Fasn* by GLT, and transfection with miR-642a-3p was unable to rescue its expression. In the case of *Cat*, compared with the control, there was a significant upregulation upon exposure to GLT which was further enhanced upon transfection with miR-642a-3p. In the case of *Txnip*, our results showed no significant changes in expression upon exposure to GLT, whereas transfection with miR-642a-3p led to a significant increase in *Txnip* expression. Finally, compared with the control, we observed a downregulation of *Pax6* by GLT which was rescued upon transfection with miR-642a-3p. Given the crucial role of glucagon-like peptide-1 receptor (Glp1r) in β cell survival and proliferation,[27] we showed that transfection of β cells with miR-642a-3p, in the presence of GLT, led to a significant upregulation of *Glp1r* (Figures S7A–S7D).

Considering that miR-642a-3p protects β cells from GICD, and since the PI3K signaling pathway—a well-established pro-survival pathway—was shown to be modulated in GO enrichment analysis, we further dissected the role of this pathway. Compared with the control, our results showed that transfection of β cells with miR-642a-3p downregulated PTEN expression and increased the phosphorylation of the downstream targets AKT and p44/42 MAPK, both previously downregulated by GLT exposure (Figures 4E and 4F). Interestingly, our results showed that exposure of β cells to GLT did not change the cytoplasmic/nuclear ratio of FOXO1 (a well-established AKT target) but, upon transfection of β cells with miR-642a-3p, we observed a 1.7-fold increase in cytoplasmic/nuclear ratio of FOXO1 (Figures 4G and 4H). Collectively, these findings demonstrate the capacity of miR-642a-3p to modulate classical pro-survival pathways ultimately protecting β cells from GICD.

miR-642a-3p increases lipid accumulation in β cells

We investigated whether PA influences cellular lipid dynamics and if the protective effects observed upon transfection of β cells with miR-642a-3p could involve changes in lipid metabolism. Compared with the control, our results demonstrated a statistically significant increase (3.8-fold) in LD accumulation upon exposure of miR-642a-3p transfected β cells to GLT (Figures 5A and 5B). We also showed that exposure of β cells to GLT in the presence of oleate recapitulated the increase in LD accumulation observed upon transfection with miR-642a-3p. Of note, LD accumulation did not increase in β cells exposed to 0.5 mM PA and 25 mM glucose. Given the involvement of *Plin2* and *Plin5* in lipid metabolism,[28] we decided to analyze their expression in our RNA-seq dataset. Our results showed that, compared with the control, miR-642a-3p increased the expression of *Plin2* and *Plin5* (Figure 5C). Taken together, these results suggest that both oleate and miR-642a-3p exert a protective effect on β cells exposed to GLT, likely by improving their capacity to accumulate lipids intracellularly. Similarly to the results obtained for miR-642a-3p, the increase in lipid accumulation by oleate was accompanied by an increase in cell survival (Figure 5D).

miRNA-mediated protection in pancreas and liver of hypercaloric-fed mice

The selection of GLT-protective miRNAs identified in our screening for further experiments was guided by comprehensive literature mining of the transcriptome and proteome datasets from PA-treated INS1E cells and/or human islet preparations.[8,29,30] We investigated the expression of miR-17-5p, miR-20a-5p, miR-20b-5p, and miR-432-5p in the pancreas and liver of mice fed with a hypercaloric diet (Figures 6A and S8). Overall, our results showed that, compared with control mice, the expression of the selected miRNAs was downregulated, without reaching statistical significance, in mice fed with a hypercaloric diet, both in the liver and pancreas (Figures 6B and 6C). These results suggest that mice fed with a hypercaloric diet showed a reduction in the levels of GLT-protective miRNAs. Since miR-642-3p

miR-642a-3p vs. GLT performed with 701 genes (115 downregulated and 586 upregulated). (G) GO:BP and KEGG pathways for genes upregulated by miR-642a-3p. (H) GO:BP and KEGG pathways for genes downregulated by miR-642a-3p. (I) Common putative targets for miR642a-3p. (J) qRT-PCR quantification of the expression of miR-642a-3p putative targets. (K) Metabolic activity following siRNA-mediated knockdown of *Cmtm6*, *Dusp4*, *Wrd13*, *Dnajc27*, and *Zdhhc7* followed by exposure to GLT. Statistical analysis was determined using one-way ANOVA, followed by Tukey's multiple comparison test. $^{*}p < 0.045$, $^{**}p < 0.0066$, $^{***}p = 0.0002$, $^{****}p < 0.0001$. The results are presented as mean ± SD (n = 3 biological replicates).

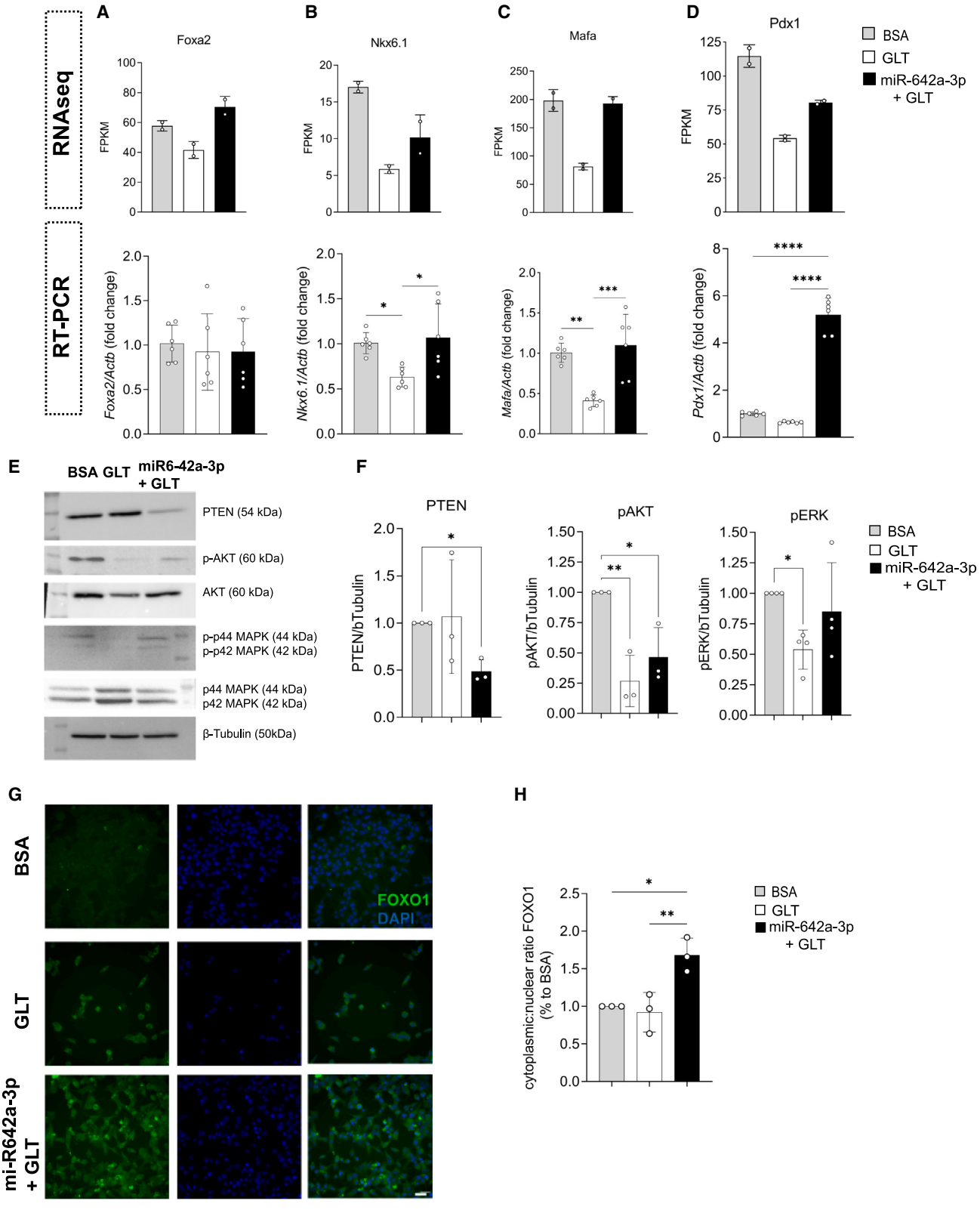

(legend on next page)

is not conserved in mice, we analyzed publicly available datasets to assess its expression in human islets from control and T2DM donors.[31,32] Analysis of two independent datasets revealed a downregulation of miR-642-3p in T2DM-derived islets, supporting our findings that it may play a protective role in this context (Figure 6D).

miRNA-extracellular vesicles signature in plasma of patients with obesity undergoing BS

Given that GLT leads to β cell dysfunction and death, phenomena frequently associated with obese and/or diabetic patients, we analyzed the expression of the same five GLT-protective miRNAs mentioned above (miR-642a-3p, miR-17-5p, miR-20a-5p, miR-20b-5p, and miR-432-5p) in extracellular vesicles (EVs) isolated from the plasma of patients undergoing BS (Figures 7A and S9). Our results showed that, before surgery, the diabetic group had 7.25% Hb_{A1c}, whereas the non-diabetic group had 5.6%. As expected, BS resulted in a reduction in BMI, decreasing from 44.62 before surgery to 35.48 kg/m^2 1 month post-surgery (Figure 7B).

Importantly, our results showed that, before surgery, obese non-diabetic patients exhibited higher levels of GLT-protective miRNAs in plasma-derived EVs in contrast to their obese diabetic counterparts. Moreover, the number of copies of miR-642a-3p per EV were statistically significant higher in non-diabetic patients ($1.26 \times 10^{-5} \pm 2.05 \times 10^{-5}$) compared with diabetic patients ($1.65 \times 10^{-6} \pm 2.81 \times 10^{-6}$) before surgery. Interestingly, for both groups of patients, there was an increase in the expression of GLT-protective miRNAs between pre-surgery and 1 month after surgery (Figure 7C). Overall, these results may suggest that elevated levels of GLT-protective miRNAs play a protective role in obese patients against diabetes.

DISCUSSION

Using an unbiased screening we identified, for the first time, miR-642a-3p as a miRNA capable of protecting β cells (and ECs) from GICD and restoring GLT-induced changes in insulin secretion as well as the expression of β cell identity genes. In hypercaloric-fed mice, we showed a reduction in the expression of GLT-protective miRNAs, whereas in obese patients we showed that the expression of these GLT-protective miRNAs was increased in obese non-diabetic patients (compared with obese and diabetic). Overall, our findings suggest a protective role for the miRNAs identified in our screening.

High glucose levels and PA act synergistically to worsen β cell function, ultimately leading to β cell death, which might in part explain the link between obesity and T2DM.[1,33] Previous studies have shown dysregulation of the miRNA landscape in obesity and T2DM.[34,35] Liu et al. reported that mice lacking miR-21 developed glucose intolerance due to impaired GSIS, but the liposome-mediated delivery of miR-21 to the pancreas of db/db mice was shown to promote Glut2 expression and reduce blood glucose levels.[36] Also, miR-17-5p was found to be downregulated in the plasma of rats fed with a high-fat and high-sugar diet.[37] However, there is a lack of consensus regarding which miRNAs can be used as biomarkers for T2DM and/or which ones can be used therapeutically to rescue/ameliorate disease course. This is mostly due to a diversity of diabetic and/or obese disease models as well as different methods to isolate and analyze the expression of selected miRNAs. For example, elevated levels of miR-146a were found in plasma[38] of T2DM patients, whereas other study indicated lower levels of miR-146a in the serum.[39]

To overcome these limitations, we used an unbiased approach and screened a library of 2,080 miRNAs to identify miRNAs capable of protecting β cells from GICD. Since implementing an assay to evaluate β cell function in an HTS format poses considerable challenges, we decided to evaluate the impact of each individual miRNA on β cell survival. Out of the 7 miRNAs identified, we explored in detail miR-642a-3p, since we recently showed that this miRNA was also able to enhance the survival of EC exposed to ischemic conditions.[26] Moreover, previous work showed that miR-642a-3p was an adipocyte-specific miRNA that actively promotes adipogenesis making it an appealing target to explore in the context of GLT.[40] Research conducted in rodent and human islets showed that insulin secretion was dependent on the duration of FFA exposure, with acute exposure increasing secretion and chronic exposure decreasing it.[4,41,42] Here, we showed that GLT acutely stimulates insulin secretion by β cells thereby contributing to chronic hyperinsulinemia—a hallmark feature of obese T2DM patients.[6] Functionally, we showed that miR-642a-3p decreased GLT-induced hyperinsulinemia in β cells unraveling a mechanism by which miR-642a-3p could protect β cells and preserve their function under GLT. An intriguing result was the impact of the BSA on GSIS. Similar to others, we used free fatty acid BSA in our experiments[43] and previous work has shown that acute exposure to BSA led to a reduction in GSIS, while a 4–6 h pre-incubation with FFA-free BSA increased GSIS.[44]

GLT has been shown to downregulate key β cell identity markers, including *Mafa* and *Pdx1*.[45,46] In line with previous studies, our results demonstrated that GLT significantly downregulated the expression of *Mafa* and *Nkx6.1* and that miR-642a-3p was sufficient to restore their expression. Interestingly, miR-642a-3p increased the expression of *Glp1r*, an effect typically observed solely in situations where glucose control is restored to physiological levels.[47,48]

Mechanistically, we showed that miR-642a-3p was able to enhance LD accumulation. This was supported by increased expression of

Figure 4. Effect of miR-642a-3p on the expression of genes involved in β cell identity and on the pro-survival signaling pathway

(A–D) FPKM and RT-PCR analysis of the transcription factors known to be involved in β cell identity (*Foxa2*, *Nkx6.1*, *Mafa*, and *Pdx1*). (E and F) Western blotting was used to analyze and quantify the expression of proteins known to be involved in cell survival. (G and H) Representative immunofluorescence images of FOXO1 expression in INS1E cells exposed to GLT and miR-642a-3p, and quantification of the cytoplasmatic/nuclear ratio of FOXO1, respectively. Statistical analysis was determined using one-way ANOVA, followed by Tukey's multiple comparisons test *$p < 0.03$, **$p < 0.0086$, ***$p = 0.0007$, ****$p < 0.0001$. The results are presented as mean ± SD ($n = 3$ biological replicates, each biological replicate containing three technical replicates). Scale bar, 25 μm. FPKM, fragments per kilobase of transcript per million mapped reads.

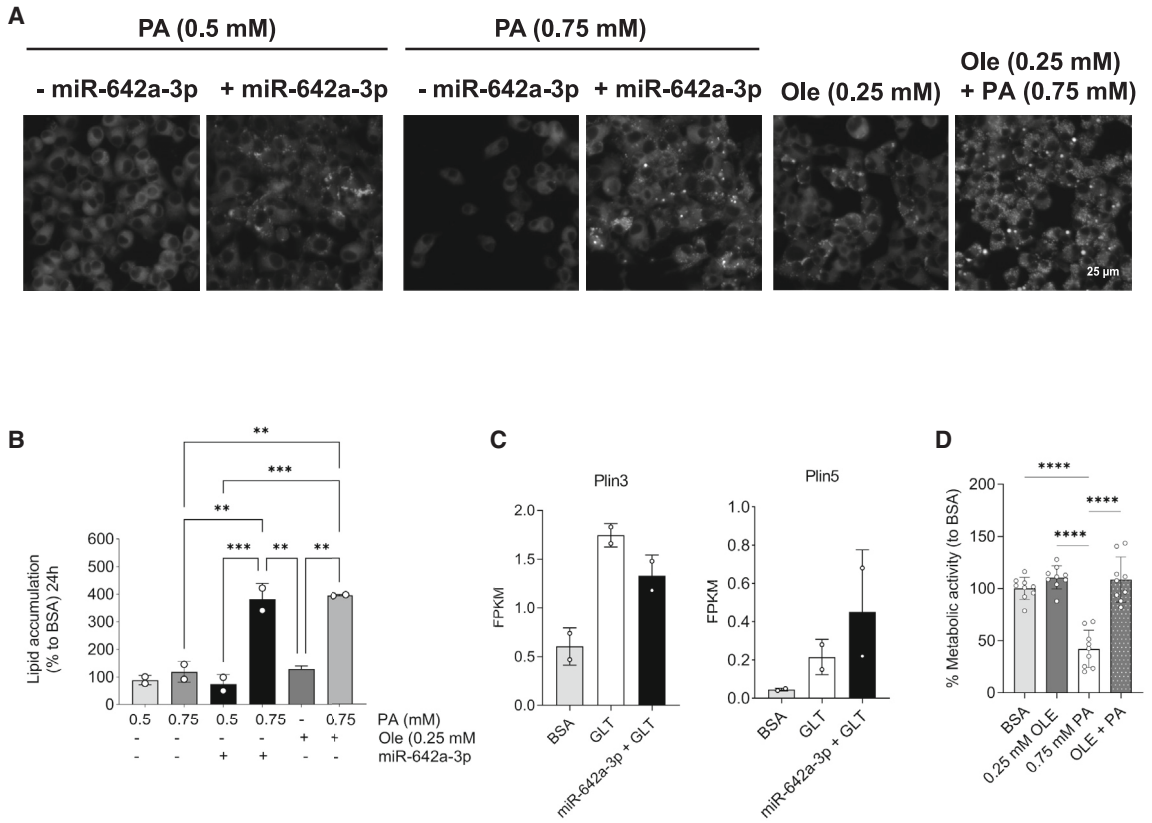

Figure 5. Effect of miR-642a-3p on lipid droplet accumulation by INS1E cells

(A and B) Representative bright-field images of INS1E cells exposed to different concentrations of fatty acids (PA, oleate, or a combination) in the presence or absence of miR-642a-3p (A) and quantification of liquid droplets (B). Cells were stained with Nile red. (C) FPKM values obtained by RNA-seq analysis for *Plin3* and *Plin5*. The results of lipid accumulation are the average of two independent experiments. Statistical analysis was determined using one-way ANOVA, followed by Tukey's multiple comparison test. $^{**}p < 0.0019$, $^{***}p < 0.0008$. (D) Metabolic activity (% to BSA) of INS1E cells cultured for 24 h with 0.25 mM oleate, 0.75 mM PA, and a combination of 0.25 mM oleate with 0.75 mM PA, in 25 mM glucose, and media containing 1% (v/v) FBS. Statistical analysis was determined using one-way ANOVA, followed by Tukey's multiple comparisons test. $^{**}p < 0.0019$, $^{***}p < 0.0008$, $^{****}p < 0.0001$. Error bars represent mean ± SD (at least two independent biological replicates were performed, each biological replicate containing three technical replicates).

Plin2 and *Plin5*, as well as upregulation of *Fasn*, a known lipid accumulation facilitator.[49] Others have shown that the extent of lipotoxicity is influenced by the fatty acid species, with oleate reported as being less lipotoxic for β cells compared with PA and other saturated fatty acids.[50,51] Moreover, Perilipin (PLIN) proteins contribute to LD structure, stability and function, with PLIN2 being shown to promote lipid storage and attenuate lipotoxicity.[28]

Upon phosphorylation by AKT, FOXO1 is translocated into the nucleus inhibiting the expression of Pdx1, a mechanism previously shown to drive apoptosis of β cells exposed to PA.[52] This suggests that the delicate equilibrium between FOXO1's retention in the cytoplasm and its translocation into the nucleus may play a pivotal role in determining whether β cells survive or succumb to the challenges posed by GLT.[10] In line with this, β cells transfected with miR-642a-3p increased the cytoplasmic/nuclear ratio of FOXO1, although we did not observe changes in the nuclear ratio of FOXO1 upon exposure to GLT.

Using RNA-seq, we identified *Akt2*, *Wdr13*, Prkab2, *Cmtm6*, *Zdhhc7*, *Dusp4*, and *Dnajc27* as putative targets of miR-642a-3p. Interestingly, these genes have previously been associated with obesity and/or proliferation of β cells in diabetes. AKT2 is a serine/threonine protein kinase important for modulating insulin sensitivity and carbohydrate metabolism.[53] In a high-fat diet-induced hepatic steatosis mouse model, AKT2 was shown to regulate obesity-induced lipid metabolic disorders in the liver and heart, and inhibition of AKT2 alleviated hepatic and cardiac injuries associated with obesity.[54] Our results showed a downregulation of *Akt2* in β cells transfected with miR-642a-3p and an increase in AKT phosphorylation at Ser473. While protein levels are primarily influenced by transcript concentrations in steady-state conditions, this relationship can be altered during stress responses, and post-transcriptional processes can cause deviations from the expected correlation between mRNA and protein expression. Other levels of regulation beyond just transcript concentration may play a role in determining protein expression levels.[55] Ablation of WDR13 in a Lepr (db/db) mouse model of diabetes

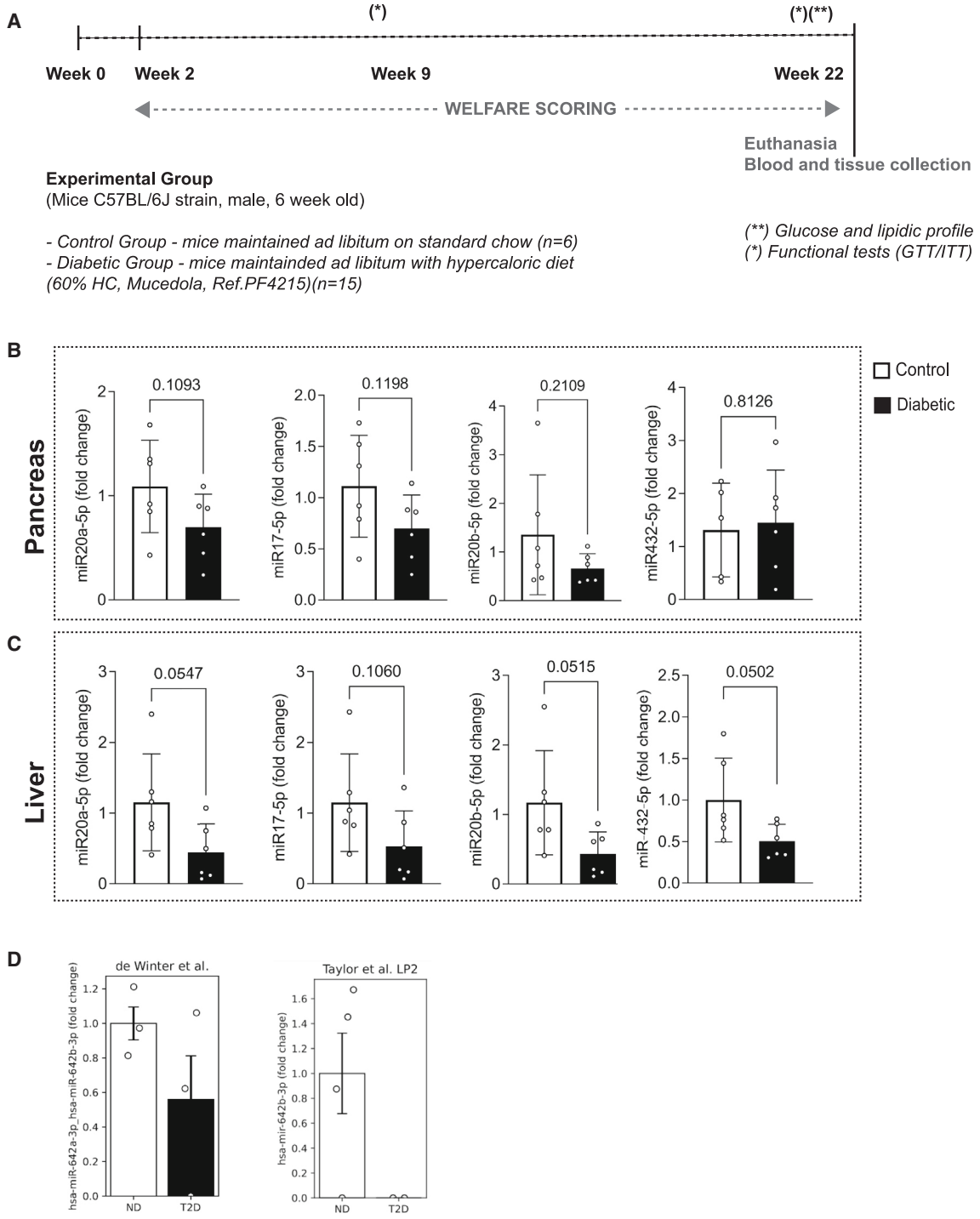

Figure 6. Expression of GLT-protective miRNAs in the pancreas and liver of mice fed with a control or hypercaloric diet

(A) Experimental graphical abstract of a mouse model of diabetes induced by a hypercaloric diet. (B) Pancreatic and (C) hepatic expression of miR-20a-5p, miR17-5p, miR-20b-5p, and miR-432-5p. (D) Expression analysis of miR-642a-3p in human pancreatic islets from control (ND) and T2DM donors (T2D). Statistical analysis was determined using unpaired t test. *$p = 0.0324$. Error bars represent SD.

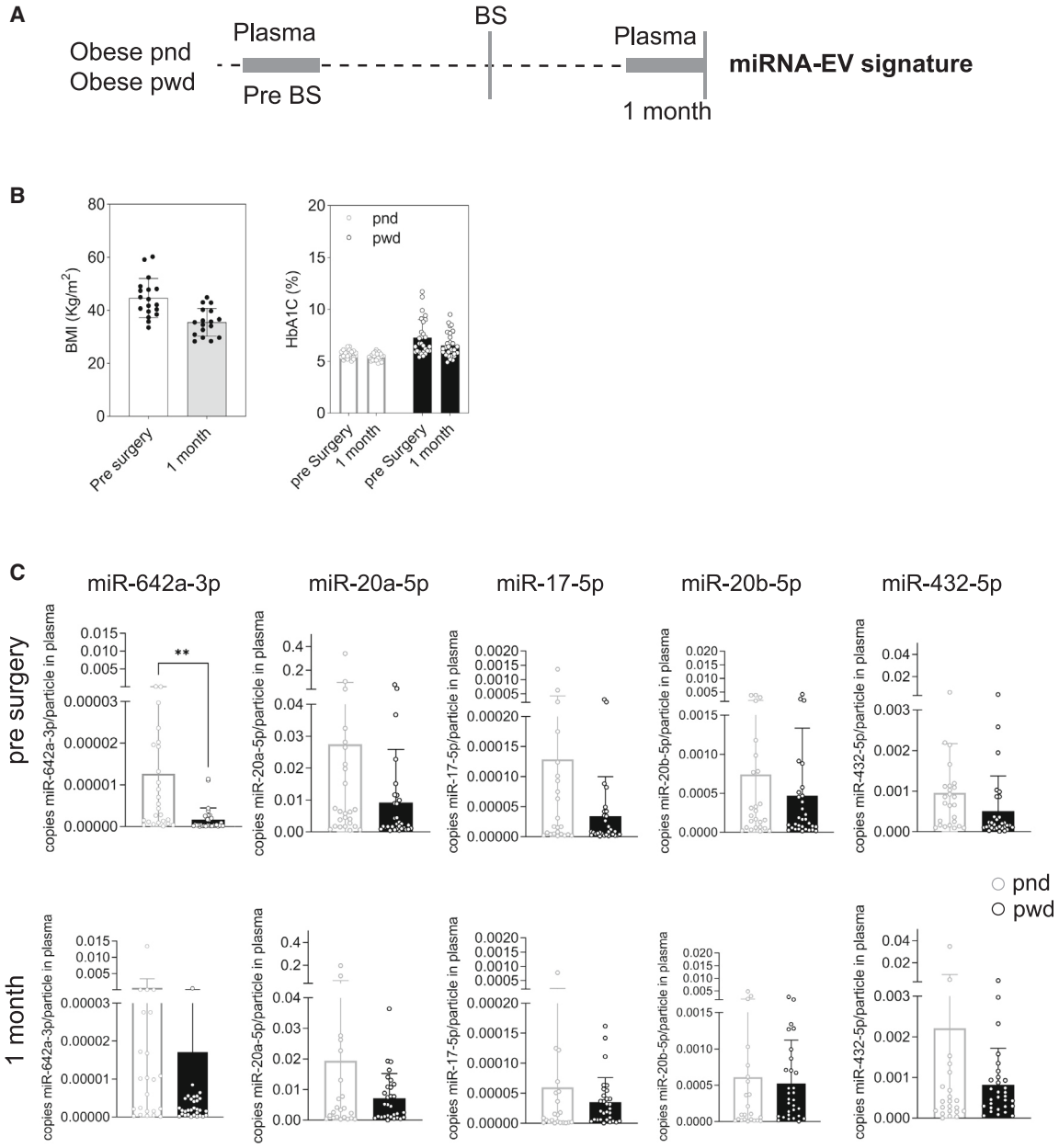

Figure 7. miRNA signature from plasma-derived EVs of obese patients selected for BS

(A) Schematic overview of sample collection. (B) Patient BMI and HbA_{1c} before and after BS. (C) Copies of miR-642a-3p, miR-20a-5p, miR17-5p, miR-20b-5p, and miR-432-5p per EV particle in plasma. Statistical analyses was performed using t test. $^{**}p = 0.0041$. Results are presented as mean ± SEM. BMI, body mass index; HbA1C, glycated hemoglobin; pnd, people non-diabetic; pwd, people with diabetes.

resulted in a significant increase in islet mass due to β cell proliferation.[56] Zinc finger DHHC-type palmitoyltransferase 7 (*Zdhhc7*) plays a crucial role in the covalent attachment of palmitic acid (palmitoylation) to target proteins.[57] DnaJ/HSP40 homolog, subfamily C, member 27 gene (*Dnajc27*), was shown to be upregulated in peripheral blood mononuclear cells and adipose tissue of obese individuals and it was linked to dysregulation of leptin and resistin.[58] DUSP4 inhibits the ERK pathway by inhibiting ERK1/2, suggesting a role in controlling cell proliferation and survival. Moreover, it has been shown that DUSP4 protects podocytes against oxidative stress and reduced DUSP4 expression impairs insulin signaling, contributing to insulin resistance in diabetic nephropathy.[59] Despite their potential role in diabetes, we showed that inhibition of these genes with siRNA did not phenocopy the survival effect observed with miR-642a-3p. On

the other hand, inhibition of *Cmtm6*, a gene belonging to a relatively understudied gene superfamily, known as the chemokine-like factor family, was able to phenocopy the effects observed with miR-642a-3p. Previous studies have shown that *Cmtm6* maintained the persistent expression of PD-L1 preventing its degradation by ubiquitination[60] and, interestingly, that the reduction of *Cmtm6* in macrophages has been linked to a decrease in LDL uptake, suggesting a pivotal role in lipid metabolism.[61] Interestingly, the knockdown of *Cmtm6* led to an upregulation of *Pdx1*, although the exact mechanism by which the inhibition led to the upregulation remains to be studied.

Mice fed with diets rich in fat and sugar exhibit a gradual onset of features associated with GLT.[62] Changes in the miRNA expression profile secondary to excessive intake of fat and sugar may contribute to the overall metabolic dysfunction in tissues other than β cells, including the liver—a critical organ in the regulation of both glucose and lipid metabolism.[59] A high-fat diet was linked to downregulation of miR-122 and upregulation of miR-200a, miR-200b, and miR-429 in the liver.[63] Here, we observe a trend toward decreased expression of GLT-protective miRNAs, suggesting that low levels could be involved in the loss of metabolic control. Notably, we demonstrated that miR-642a-3p expression was downregulated in human islets isolated from T2DM patients compared with non-diabetic controls.

Multiple studies have investigated how the miRNAs' signatures, including exosomal-derived miRNAs, are associated with obesity and how BS affects their expression.[22] Bae et al. reported that BS altered exosomal miRNA expression and identified a set of nine miRNAs that were associated with obesity and responsive to the surgical treatment.[64] The study of miRNAs expressed in patient-derived samples is often constrained by a limited sample size and by the use of miRNA microarrays that analyze only a restricted number of miRNAs.[34] Although these limitations frequently result in a lack of consensus, a systematic summary of studies comparing miRNA expression levels before and after BS was performed and 13 miRNAs, reported in at least two human studies, were found to have the same direction of modulation (downregulated: hsa-miR-93-5p, hsa-miR-106b-5p, hsa-let-7b-5p, hsa-let-7i-5p, hsa-miR-16-5p, hsa-miR-19b-3p, hsa-miR-92a-3p, hsa-miR-222-3p, hsa-miR-142-3p, hsa-miR-140-5p, hsa-miR-155-5p; upregulated: hsa-miR-7-5p, hsa-miR-320c).[22] Given these discrepancies, and since exosomal miRNAs are protected from extracellular RNases, we analyzed the expression of GLT-protective miRNAs identified in our screening in EVs isolated from plasma of patients undergoing BS. We showed that, before surgery, the expression of miR-642a-3p was significantly higher in non-diabetic patients compared with their diabetic counterparts, suggesting that the higher levels of miR-642a-3p in the non-diabetic patients could have contributed to the preservation of their β cells despite their obesity. The results presented herein suggest that profiling exosomal miRNAs in the context of obesity and/or metabolic syndrome could be used to identify patients at risk and, more importantly, miRNA-based therapies could be a novel therapeutic strategy for obese and/or diabetic patients. In fact, it has been shown that plasma-derived EVs from obese mice promoted glucose intolerance and dyslipidemia when injected into lean mice for 4 weeks. Furthermore, the same metabolic effects were obtained by treating control mice with EVs obtained from control mice previously transfected with four miRNA mimics known to be upregulated in obese mice: miR-122, miR-192, miR-27a-3p, and miR-27b-3p.[65] Further preclinical studies are essential to unravel the potential applications of miRNA-based therapies. Bioengineered EVs, designed to enhance bioactivity, biodistribution, and targeted delivery to the pancreas, present promising candidates for addressing diabetes and obesity.[66] In the context of pancreatic β cell delivery, we could envision the use of delivery systems (i.e., EV, lipid nanoparticles, hydrogels) functionalized with GLP1 agonists/antagonists (targeting) and/or miRNAs (bioactivity). Limitations of this study include the following: (1) the use of a rat cell line instead of a human cell line, since some studies suggest that PA did not significantly affect apoptosis,[67] (2) with no access to human-derived islets, we mostly used rat insulinoma cell lines to unravel the mechanisms governing GLT and the protective effect of miR-642a-3p, (3) the *in vivo* analysis of miRNA expression in the pancreas is limited in its ability to pinpoint the specific impact on β cells, as the full pancreas was processed, making it impossible to determine the contribution of individual cell types, (4) the plasma EVs (pEVs) isolated might have been contaminated with other non-vesicular structures/proteins and therefore the results obtained need to be further confirmed using EVs isolated and/or purified using different methods.

In conclusion, the present study identified miR-642a-3p as a miRNA capable of rescuing β cells from GICD. Mechanistic studies showed that miR-642a-3p restored the expression of β cell identity genes and rescued β cell function. In hypercaloric-fed mice and patients subjected to BS, we showed an upregulation of GLT-protective miRNAs in non-diabetic mice and patients.

This is the first study showing that miR-642a-3p protects β cells from GLT-induced dysfunction and cell death.

MATERIALS AND METHODS

Cell culture

INS1E cell line was cultured in RPMI 1640, supplemented with 10% (v/v) FBS (no. 10270106, Gibco), 50 U/mL penicillin, 50 μg/mL streptomycin, 10 mM HEPES, 1 mM sodium pyruvate, 50 μM β-mercaptoethanol, and maintained in 5% CO_2 at 37°C. Cells were used between passages 61 and 72 and were tested regularly for mycoplasma infection, using Mycoalert mycoplasma detection kit (no. LT07-418), Lonza, according to the manufacturer's instructions.

PA in BSA-containing medium

Sodium palmitate (no. P9767, Sigma-Aldrich, St. Louis, MO) was prepared at 50 mM stock concentration in 90% (v/v) ethanol, heated at 60°C until dissolved and diluted to a final concentration of 0.75% (v/v) fatty acid-free BSA-containing medium (no. 3117057001, Roche), in 11 or 25 mM glucose. Control for equal amounts of ethanol were tested.

GLT assay

PA stock was diluted in 0.75% (v/v) fatty acid-free BSA-containing RPMI 1640 media (no. 3117057001, Roche), with either 11 or 25 mM glucose, as before.[43]

Next, 4×10^4 INS1E cells were seeded in a flat-bottom 96-well plate (no. 734-1662, Corning, NY) in RPMI 1640, supplemented with 10% (v/v) FBS (no. 10270106, Gibco), 50 U/mL penicillin, 50 μg/mL streptomycin, 10 mM HEPES, 1 mM sodium pyruvate, 50 μM β-mercaptoethanol, for 24 h before adding increasing concentrations of PA, for another 24 h.

Cell metabolic activity assay

After being subject to different treatments, cell metabolic activity was evaluated through resazurin reduction assay (Invitrogen, Waltham, MA) according to the manufacturer's instructions.[68] In brief, the medium was replaced with RPMI supplemented with 10% (v/v) FBS, 50 U/mL penicillin, 50 μg/mL streptomycin, and 10 μg/mL resazurin. Cells were incubated for 1–2 h at 37°C and 5% of CO_2 upon which fluorescence was measured (540 nm excitation and 590 nm emission) using the microplate reader Synergy H1 (BioTek Instruments, Winooski, VT).

Cell mass (sulforhodamine B) assay

The sulforhodamine B (SRB) assay is based on the measurement of cellular protein content.[25] In brief, after applying different treatments, cells were fixed with 1% (v/v) acetic acid in methanol for 18 h at −20°C, upon which the fixation solution was removed, and the plates dried at 37°C for 1–2 h. Next, 150 μL of 0.05% (v/v) SRB solution was added to the wells and incubated at 37°C for 1 h upon which the wells were washed with 1% (v/v) acetic acid in water and dried. Then, 10 mM Tris (pH 10) was added and the plates were stirred for 15 min and optical density was measured (540 nm) using the microplate reader Synergy H1 (BioTek Instruments).

HTS assay

INS1E (4×10^4 cells) were reverse transfected in a 96-well plate with a library of miRNAmimics (Dharmacon miRIDIAN miRNA Library—Human mimic miRBase version 19.0; 2,080 miR mimics) according to the manufacturer's instructions. Per well, complexes of miRNA:Lipofectamine RNAiMAX (Thermo Fisher Scientific, no. 13778) were prepared with 50 nM miRNA and 0.3 μL Lipofectamine RNAiMAX in OptiMEM medium (Gibco, no. 51985-026) in a final volume of 100 μL. Complexes were allowed to form during 30 min at room temperature. Lipofectamine RNAiMAX-treated cells were used as a control.[26] After the incubation, INS1E cells were added to the well and transfection was allowed to proceed for 48 h, upon which the GLT stimulus (0.75 mM PA, 25 mM glucose, 1% FBS [v/v]) was added for further 24 h. After 24 h we evaluated the metabolic activity and cell mass and a bright-field image was acquired for each individually transfected miRNA using the InCell Analyzer 2200 automated high-content imager (GE Healthcare) at 40× magnification.

GSIS and insulin levels by ELISA

INS1E (4×10^4 cells) were reverse transfected in a 96-well plate with 50 nM miR-642a-3p for 48 h and exposed to GLT conditions (0.75 mM PA, 25 mM glucose, 1% FBS [v/v]) for 24 h. Afterward, supernatant were used to quantify the degree of GSIS. In brief, to enhance the sensitivity of INS1E cells to a high-glucose challenge, cells were washed in Krebs-Ringer solution (KRB) (HEPES-buffered, no. J67795.AP, Alfa Aesar) supplemented with 120 mM NaCl, 5 mM KCl, 1 mM $MgCl_2$, 5.5 mM HEPES, 2 mM $CaCl_2$, 25 mM $NaHCO_3$, 1 mM glucose (pH 7.2) supplemented with 0.5% (v/v) BSA.[69,70] Subsequently, cells were incubated in KRB low glucose (1.67 mM) for 1 h, washed, another 1 h in KRB high glucose (16.7 mM), washed 3 times, and finally 1 h in KRB low glucose (1.67 mM). Samples were collected between each treatment, centrifuged at 300 × *g* for 3 min and the supernatant was stored at −20°C for subsequent analysis. Secretion of insulin was measured using the High Range Rat Insulin enzyme-linked immunosorbent assay (ELISA) (no. 10-1145-01, Mercodia, Uppsala, Sweden), according to the manufacturer's recommendations. In brief, 10 μL of each of the calibrators, controls, and samples were pipetted into a mouse monoclonal anti-insulin-coated plate and 50 μL of enzyme conjugate 1× solution was added and incubated on a plate shaker (700–900 rpm) for 2 h at room temperature (18°C–25°C). Afterward, the wells were washed 6 times with 350 μL wash buffer 1× solution, 200 μL TMB substrate was added per well and incubated for 15 min on the bench at room temperature (18°C–25°C). Finally, 50 μL Stop Solution was added to each well, the plate was placed on the shaker for approximately 5 s to ensure mixing, and the optical density was read at 450 nm. The amount of insulin secreted was normalized for the total protein content.

siRNA-mediated knockdown

INS1E (4×10^4 cells) were reverse transfected in a 96-well plate with siRNA pre-designed to target specific genes (IDT, Coralville). Per well, complexes of siRNA:Lipofectamine RNAiMAX (Thermo Fisher Scientific, no. 13778) were prepared using 50 nM siRNA and 0.3 μL Lipofectamine RNAiMAX in OptiMEM medium (Gibco, no. 51985-026) in a final volume of 100 μL. Complexes were allowed to form during 30 min at room temperature. Lipofectamine RNAiMAX-treated cells were used as a control.[26] After the incubation, INS1E cells were added to the well and transfection was allowed to proceed for 48 h, upon which the GLT stimulus (0.75 mM PA, 25 mM glucose, 1% FBS [v/v]), was added for further 24 h. After 24 h we evaluated the metabolic activity and evaluated β cell identity markers by RT-PCR.

Immunofluorescence microscopy

INS1E (4×10^4 cells) were reverse transfected with 50 nM of miR-642a-3p for 48 h and exposed to GLT conditions (0.75 mM PA, 25 mM glucose, 1% FBS [v/v]), for 24 h. Afterward, cells were washed with 100 μL PBS and fixed with 50 μL 4% (v/v) paraformaldehyde for 10–20 min at room temperature. Next, cells were permeabilized using 0.2% (v/v) Triton X-100 for 10–20 min at room temperature. To block non-specific interactions, cells were incubated in 1% (v/v) BSA, with 5% (v/v) normal goat serum and 0.3% (v/v) Triton X-100 in PBS, for

45 min. The following primary antibodies were used: insulin (1:50; FLEX Polyclonal Guinea Pig Anti Insulin [no. IR00261-2, Agilent], FOXO1 [1:100, C29H4] Rabbit mAb [no. 1672880S, Cell Signaling Technology]) and Rabbit Polyclonal GLP-1R Antibody (1:250; NBP1-97308SS, Novus Biologicals). All the antibodies were diluted in PBS with 1% (v/v) BSA and 0.3% (v/v) Triton X-100 and incubated for 1 h at room temperature. Subsequently, cells were washed and incubated with secondary Alexa 568 anti-guinea pig (1:1,000) or Alexa 488 anti-rabbit (1:1,000), diluted in a PBS solution containing 1% (v/v) BSA and 0.3% (v/v) Triton X-100 for 1 h at room temperature. Finally, the nuclei were stained with DAPI (1 μg/mL) for 10 min at room temperature. Randomly, 8 fields per well were selected for image acquisition using the InCell Analyzer 2200 automated high-content imager (GE Healthcare) using 40× magnification. InCell Investigator software (GE Healthcare) was used for quantification. Cytosolic and nuclear FOXO1 were resolved by following an image-based segmentation strategy using InCell Investigator software (GE Healthcare).

Western blotting

INS1E (4×10^4 cells) were reverse transfected with 50 nM miR-642a-3p for 48 h and exposed to GLT conditions (0.75 mM PA, 25 mM glucose, 1% FBS [v/v]) for 24 h. Afterward, cells were gently washed with PBS, lysed in RIPA Lysis Buffer containing 100× protease/phosphatase inhibitor cocktail (no. 5872, Cell Signaling), vortexed, and kept on ice for 30 min. The supernatant was collected after centrifugation at 13,000 rpm for 15 min. Protein was quantified by the microBCA method using BSA as a standard (no. 23235, Thermo Fisher Scientific). Protein samples (20–50 μg) were separated by electrophoresis using 12% (v/v) sodium dodecyl sulfate (SDS)-polyacrylamide gels. After electrophoresis, the proteins were transferred onto PVDF membranes (Millipore, Billerica, MA). The membranes were blocked in 5% (v/v) BSA (Roche, Basel, Switzerland) in Tris-buffered saline-Tween at room temperature for 60 min. The following antibodies were incubated overnight at 4°C: Rabbit Polyclonal p-AKT Antibody (1:500; no. 4060s, Cell Signaling), Rabbit Polyclonal AKT Antibody (1:500; no. 4691S, Cell Signaling), Rabbit Polyclonal Phospho-p44/42 MAPK Antibody (Erk1/2) (1:500; no. 4376S, Cell Signaling), Rabbit Polyclonal p44/42 MAPK (Erk1/2) Antibody (1:500; 4695S, Cell Signaling), Mouse polyclonal β-tubulin Antibody (1:5,000; no. T8328, Sigma-Aldrich), Rabbit Polyclonal GLP-1R Antibody (1:250; NBP1-97308SS, Novus Biologicals). Next, the membranes were incubated at room temperature for 60 min with anti-rabbit-HRP-conjugated (1:5,000; Cell Signaling Technology) or anti-goat-HRP-conjugated secondary antibody (1:5,000; Cell Signaling). Blots were imaged using a Biospectrum-Multispectral imaging system (UVP; LLC Upland, CA; Cambridge, UK) and the densities of each band were calculated with Quantity one software (Bio-Rad).

Nile red

Lipid accumulation was assessed by Nile red staining assay, as previously described.[68] In brief, a 1:200 dilution from Nile red was prepared from the stock (0.5 mg/mL in acetone) in medium without FBS and 100 μL of this solution was added to the cells for 1 h in the dark at 37°C. Subsequently, the lipid content was measured fluorimetrically (excitation: 520 nm; emission: 620 nm) using the microplate reader Synergy H1 (BioTek Instruments). The percentage of lipid accumulation was normalized to the nuclear counts. Images of the stained cells were acquired using InCell Analyzer 2200 automated high-content imager (GE Healthcare) at 40× magnification.

RT-PCR

INS1E (4×10^4 cells) were reverse transfected with 50 nM miR-642a-3p for 48 h and exposed to GLT conditions (0.75 mM PA, 25 mM glucose, 1% FBS [v/v]), for 24 h. Afterward, cells were lysed and RNA was isolated using a RNeasy Micro Kit (no. 50974034, QIAGEN, Hilden, Germany) according to the manufacturer's instructions and quantified on a spectrophotometer. Next, 500 ng of RNA was reverse transcribed using a qScript SuperMix kit (no. 95048; Quantabio, MA) and the obtained cDNA was used to quantify the mRNA expression of target genes using quantitative real-time PCR analysis. For this, PCR products were amplified using the NZYSpeedy qPCR Green Master Mix kit (no. MB22403, NZYtech, Lisbon, Portugal) according to the manufacturer's recommendations. The housekeeping gene *Actb* was used for normalization and fold changes were determined using the $2^{-\Delta\Delta Ct}$ method.[71] Primer sequences are available in Table S9.

RNA-seq and data analysis

INS1E (4×10^4 cells) were reverse transfected with 50 nM miR-642a-3p for 48 h and exposed to GLT conditions (0.75 mM PA, 25 mM glucose, 1% FBS [v/v]), for 24 h ($n = 2$). Afterward, cells were lysed and RNA was isolated using a RNeasy Micro Kit (no. 50974034, QIAGEN) according to the manufacturer's instructions and quantified on a spectrophotometer. Two biological replicates were performed. The mRNA library construction was done with different steps: (1) the oligo dT selection (mRNA enrichment) was done using oligo dT beads to enrich mRNA with a poly(A) tail, (2) the fragment the RNA and first-strand cDNA was generated using random N6-primed reverse transcription, followed by second-strand cDNA synthesis with dUTP instead of dTTP, (3) the synthesized cDNA was subjected to end-repair, 3′ adenylated and adaptors were ligated to the ends of these 3′ adenylated cDNA fragments, (4) before PCR amplification, the dUTP-marked strand was selectively degraded by uracil-DNA-glycosylase and the remaining strand was amplified to generate a cDNA library suitable for sequencing. Multiple rounds of PCR amplification were performed to enrich the purified cDNA template using PCR primer; the PCR product was heat denatured, the single-strand DNA was cyclized by splint oligo and DNA ligase followed by a DNA nanoball synthesis and sequencing on DNBSEQ (DNBSEQ Technology) platform. Subsequent analysis were performed after the filtered clean reads were aligned to the reference sequence. The sequencing data filtering was done using the software SOAPnuke.[72] Hierarchical Indexing for Spliced Alignment of Transcripts (HISAT) was the software used for mapping RNA-seq reads[73] and significantly up- and downregulated genes (differentially expressed) were selected based on criteria described below.

Filtering criteria

Compared with the control (Lipofectamine-treated cells), transfection of β cells with 50 nM miR-642a-3p for 48 h resulted in a total of 7,495 DEG (3,538 upregulated and 3,921 downregulated). We further filtered this list based on genes with a log2FC > |1| and FPKM > 1 for each of the replicas of one of the conditions, ending up with 1,381 genes (903 downregulated and 478 upregulated) (Table S5).

To analyze the transcriptional changes induced by GLT on β cells, volcano plots were constructed with the applied criteria log2FC > |1|, resulting in 3,950 genes. From this list, we selected genes with a log2FC > |2| and FPKM > 1 for each of the replicas of one of the conditions, ending up with 622 genes (412 downregulated and 210 upregulated) to build the heatmap (Table S3).

To analyze the transcriptional changes induced by miR-642a-3p on β cells, volcano plots were constructed with selected genes with a log2FC > |1|, resulting in 4,069 genes and, from this list, we selected genes with a log2FC > |2| and FPKM > 1 for each of the replicas of one of the conditions ending up with 701 genes (586 upregulated and 115 downregulated) to build the heatmap (Table S4).

Targets of the miR-642a-3p: we focused our analysis on genes downregulated by miR-642a-3p (903 genes). To that end, we selected genes with an FPKM > 1 for each of the replicas of one of the conditions and a log2FC > |1.5| and ended up with a list of 238 genes (Table S6).

miR-642 binding conservation

Genome FASTA and GTF files were retrieved from the Ensembl database for human (Homo sapiens GRCh38, Ensembl GTF version 113), mouse (Mus musculus GRCm39, Ensembl GTF version 113), and rat (Rattus norvegicus mRatBN7.2, Ensembl GTF version 113). Mature miRNA sequences for hsa-miR-642a-3p in FASTA format were downloaded from miRbase (release 22.1).[74] For each species, the chromosome position and strand orientation of the Cmtm6 3′ UTR were extracted from the GTF file, and the output was saved into a BED file. A FASTA file with the full-length 3′ UTR sequences was made by using bedtools (version 2.30.0) getfasta with the option -s to force the strandedness. miRNA binding scores were computed using the miRanda software,[75] with the miRNA FASTA and 3′ UTR FASTAs as input. The settings applied were: score threshold of 140, energy threshold of 1 kcal/mol, scaling parameter of 4, gap-open penalty of −4, and gap-extend penalty of −9. Sequence conservation between the human, mouse, and rat 3′ UTRs was performed in python, using needle pairwise sequence alignment (emboss version 6.6.0.0; psa version 1.0.1). Sequence conservation, miRNA binding scores, and binding position for each species were visualized using pygenomeviz (version 1.3.0). Code is available at https://github.com/tjj-dewinter/miRNA_conservation.

GLT-protective miRNA selection

The GLT-protective miRNA selection was based on literature mining of the transcriptome and proteome of PA-treated INS1E cells and/or human islets preparations (Table S4). We identified 17 miRNAs using HTS and selected 5 (miR-642a-3p, miR-20a-5p, miR-17-5p, miR-20b-5p, and miR-432-5p) based on their capacity to target a high number of differentially expressed genes. Other miRNAs were disregarded due to their low expression in pEVs of patients undergoing BS.

Bariatric cohort

Study population

All samples were obtained from patients from the surgery department of the Centro Hospitalar e Universitário de Santo António (CHUdSA) after receiving an informed consent. This study was approved by the Ethics Commission of the CHUdSA with the reference number 2020-075 (060-DEFI. 061-CE). With support from our National Health Service facilities and adherence to the established project protocol, no costs were incurred by the patient.

Sampling

To obtain plasma, blood samples were collected from each patient in a labeled EDTA tube. Centrifugation was performed at 15,000 × *g* for 10 min at 4°C and the supernatant was stored at −80°C until use.

Animal study

Animal experiments were conducted in compliant with the Animal Care National and European Directives. The project received approval (no. 3/2022) from the local animal welfare body (ORBEA). The animal study was performed in a mouse model of diabetes induced by a hypercaloric diet, using 13, 6-week-old male mice (C57BL/6J strain) purchased from Charles-River and maintained in the Coimbra Institute for Clinical and Biomedical Research (iCBR) animal facility at the Faculty of Medicine of the University of Coimbra (FMUC). After 2 weeks of quarantine, the animals were randomly divided into two groups. Twenty-week protocol (control group, $n = 6$): mice maintained *ad libitum* on standard chow; diabetic group ($n = 7$): mice maintained *ad libitum* with a hypercaloric diet (60% carbohydrates, Mucedola, ref. PF4215). Throughout the study, the weekly evolution of their weight was monitored. *In vivo*, glucose tolerance tests (GTTs) and insulin tolerance tests (ITTs) were performed at weeks 19 and 20 of the study. The sample size was determined with an α level set at 0.05 and a power level at 0.95. The variation in the group sizes stems from the loss of an animal in the control group during an *in vivo* experimental procedure (ITT). Measures were taken into account to follow the 3Rs principles, such as a small number of mice ($n = 7$ per group). The sample size was calculated using G*power software.). In terms of refinement, the team members that carried out the animal procedures are very experienced in *in vivo* tests (including GTT and ITT) and in *ex vivo* determinations, an appropriate species and strain was used, which allows conclusions to be drawn, a robust model was chosen, excellent conditions in terms of animal facility were available, and monitoring of animal welfare was thorough. Critical limits, such as food/water intake, weight loss weight loss of more than 15% (fluid therapy was used if necessary), and feces consistency, were monitored, and animals were humanely euthanized under deep anesthesia. Animal behavior and body appearance were also closely observed throughout the study. The animals

were sacrificed with an anesthetic overdose and blood was collected for separation into serum. Liver and pancreas were collected for miRNA profile, and immediately stored at −80°C until use.

Metabolic characterization

On the day of sacrifice, after a fasting period of 6 h, glucose levels were determined. A drop of blood was collected from the jugular vein through venipuncture and measured using an Accu-Chek Aviva glucometer (Roche, Mannheim, Germany) GTT: on week 19, mice were administered intraperitoneally with a glucose bolus of 2 g/kg BW following a 6-h fasting period. Blood glucose levels were quantified through the tail vein before the injection and 15, 30, 45, and 60 min after, using the portable Accu-Chek Aviva glucometer (Roche, Mannheim, Germany). The area under the curve (AUC) for the GTT was calculated by using the trapezoidal method, as previously described.[76]

Insulin tolerance test (ITT): on week 20, 0.75 U/kg BW of insulin was administered intraperitoneally (Actrapid Novo Nordisk) following a 6-h fasting period. A drop of blood was collected from the tail vein before the bolus and blood glucose levels were measured using the portable Accu-Chek Aviva glucometer (Roche, Mannheim, Germany) 30, 60, and 120 min thereafter. The AUC for the ITT was calculated by using the trapezoidal method.

Serum levels of total cholesterol, alanine aminotransferase, and aspartate aminotransferase were assessed by colorimetric methods using an automated analyzer (Hitachi 717, Roche Diagnostics, Mannheim, Germany).

Pancreas and liver miRNA profile by RT-PCR

Total RNA was extracted using the TRIzol reagent (Life Technologies, Carlsbad, CA) according to the manufacturer's protocol. RNA concentration and purity were determined using NanoDrop (Thermo Fisher Scientific, Waltham, MA). Next, RNA was reverse transcribed using 5× miRCURY RT reaction buffer and 10× miRCURY RT Enzyme Mix, and the obtained cDNA was used to quantify miRNA expression by quantitative real-time PCR analysis. For this, PCR products were amplified using the NZYSpeedy qPCR Green Master Mix kit (no. MB22403, NZYtech) according to the manufacturer's instructions. Normalization was done to U6 and fold changes were determined using the $2^{-\Delta\Delta Ct}$ method.

pEV isolation

Isolation of pEVs was performed as previously described with small modifications.[77] In brief, samples were centrifuged at 3,000 × *g* for 15 min to remove cells and cell debris. The supernatant was mixed with 5 U/mL human thrombin (no. T7009, Sigma-Aldrich) for 5 min and centrifuged at 10,000 × *g* for 5 min to remove fibrinogen. Next, the corresponding amount of ExoQuick (no. EXOTC10A-1, System BioSciences) was added according to the manufacturer's instructions (ratio 5:1 [v/v]), mixed, and incubated for 45 min at 4°C. Samples were centrifuged at 1,500 × *g* for 30 min, resuspended in a final volume of 150 μL, subjected to 2 μg/mL RNase (no. R4875, Sigma-Aldrich) treatment for 30 min at room temperature, and repurified again via ExoQuick. Finally, pEVs were resuspended in 150 μL of PBS and stored at −80°C.

EV characterization

Nanoparticle tracking analysis

The size and concentration of the pEVs were calculated using a NanoSight NS300 (Malvern Instruments, Malvern, UK). To obtain a reliable reading, pEVs were diluted in PBS until a value of 15–45 particles/frame was obtained. The PBS used was confirmed to be pure (<5 particles per frame). For each sample, 5 videos of 30 s were recorded with the camera level set at 13. All the videos were processed with nanoparticle tracking analysis (NTA 3.0) analytical software.[78]

Zeta potential

Surface charge of pEVs was measured using the NanoBrook ZetaPALS Potential Analyzer (Brookhaven Instruments, Long Island, NY). Per sample, 5 μL of EVs were diluted in 1,500 μL of biological-grade ultrapure water (Fisher Scientific, NH) and the EVs were placed in contact with the zeta potential electrode and allowed to stabilize for 10 min. Five runs (using the Smoluchowski module) were performed for each sample at room temperature.

Protein quantification

Quantification of the total protein of pEVs was performed using the microBCA protein assay[79] kit (Thermo Fisher Scientific) following the manufacturer's recommendations. In short, a 10-point standard curve was obtained with BSA. For disrupting the EV membrane, samples were diluted in 2% (v/v) SDS at room temperature. Then, 50 μL of the latest mix was pipetted in duplicate in a 96-well Corning Costar cell culture plate (Corning), the reaction solution was added and incubated for 2 h at 37°C. Finally, the plate was equilibrated at room temperature for 15 min and the absorbance at 562 nm was read in microplate reader Synergy H1 (BioTek, VT).

EV-miRNA signature by RT-PCR

RNA from plasma-derived EVs was isolated by miRNeasy Micro Kit (no. 217084, QIAGEN) according to the manufacturer's instructions and quantified on a spectrophotometer. Next, RNA was reverse transcribed using a 5× miRCURY RT reaction buffer and 10× miRCURY RT Enzyme Mix. The resulting cDNA was used to quantify miRNA expression by quantitative real-time PCR. For this, PCR products were amplified using the NZYSpeedy qPCR Green Master Mix kit (no. MB22403, NZYtech) according to the manufacturer's instructions. Normalization was done to *5S*. miRNA-EV signature was represented as the number of miRNA copies per particle.

Statistics

GraphPad Prism (version 9) software was used to perform statistical analysis. All experiments were performed as at least two independent experiments. Results were expressed as the mean ± SD. For statistical comparison, analysis of variance (ANOVA) or t tests were used as indicated.

ACKNOWLEDGMENTS

This work was supported by The Netherlands Organisation for Health Research and Development (ZonMW, reference 95105008), "BIO-MED: Engenharia Biomolecular de Vesículas Extracelulares para Medicina Regenerative" (reference CENTRO-01-0145-FEDER-181228), Twinning RESETAgeing (Ref:952266), SPD – Sociedade Portuguesa De Diabetologia, Grupo de Estudos de Investigação Fundamental e Translacional (GIFT), and MIA-Portugal (this project has received funding from the European Union's Horizon 2020 research and innovation programme under grant agreement no. 857524). S.S.P. was supported by FCT (SFRH/BD/144119/2019), HF CEECIND/01880/2018, CHA CEECIND/2022.00041. C.D., C.H.A., F.R., L.F., J.J., and H.F. acknowledge support from FCT/MCTES (CIBB strategic project UIDP/04539/2020) and European Union's Horizon Europe program (Excellence Hubs – HORIZON-WIDERA-2022-ACCESS-04-01), under the grant agreement #101087071.

AUTHOR CONTRIBUTIONS

S.S.P. designed and performed research, analyzed data, and wrote the manuscript. C.H.A., J.T.d.O., S.V., F.R., J.S., F.C., and T.J.J.d.W. performed research and reviewed and edited the manuscript. L.F., M.G., and M.B. reviewed and edited the manuscript. H.F. and J.J. supervised the project, designed and interpreted the research, and wrote the manuscript. All authors critically read the manuscript.

DECLARATION OF INTERESTS

The authors declare no competing interests.

SUPPLEMENTAL INFORMATION

Supplemental information can be found online at https://doi.org/10.1016/j.omtn.2025.102498.

REFERENCES

1. Eizirik, D.L., Pasquali, L., and Cnop, M. (2020). Pancreatic β-cells in type 1 and type 2 diabetes mellitus: different pathways to failure. Nat. Rev. Endocrinol. *16*, 349–362. https://doi.org/10.1038/s41574-020-0355-7.

2. Zheng, Y., Ley, S.H., and Hu, F.B. (2018). Global aetiology and epidemiology of type 2 diabetes mellitus and its complications. Nat. Rev. Endocrinol. *14*, 88–98. https://doi.org/10.1038/nrendo.2017.151.

3. Blüher, M. (2019). Obesity: global epidemiology and pathogenesis. Nat. Rev. Endocrinol. *15*, 288–298. https://doi.org/10.1038/s41574-019-0176-8.

4. Lytrivi, M., Castell, A.L., Poitout, V., and Cnop, M. (2020). Recent Insights Into Mechanisms of β-Cell Lipo- and Glucolipotoxicity in Type 2 Diabetes. J. Mol. Biol. *432*, 1514–1534. https://doi.org/10.1016/j.jmb.2019.09.016.

5. Cunha, D.A., Hekerman, P., Ladrière, L., Bazarra-Castro, A., Ortis, F., Wakeham, M.C., Moore, F., Rasschaert, J., Cardozo, A.K., Bellomo, E., et al. (2008). Initiation and execution of lipotoxic ER stress in pancreatic β-cells. J. Cell Sci. *121*, 2308–2318. https://doi.org/10.1242/jcs.026062.

6. Thomas, P., Gallagher, M.T., and Da Silva Xavier, G. (2023). Beta cell lipotoxicity in the development of type 2 diabetes: the need for species-specific understanding. Front. Endocrinol. *14*, 1275835. https://doi.org/10.3389/fendo.2023.1275835.

7. Lee, S.H., Cunha, D., Piermarocchi, C., Paternostro, G., Pinkerton, A., Ladriere, L., Marchetti, P., Eizirik, D.L., Cnop, M., and Levine, F. (2017). High-throughput screening and bioinformatic analysis to ascertain compounds that prevent saturated fatty acid-induced β-cell apoptosis. Biochem. Pharmacol. *138*, 140–149. https://doi.org/10.1016/j.bcp.2017.05.007.

8. Cnop, M., Abdulkarim, B., Bottu, G., Cunha, D.A., Igoillo-Esteve, M., Masini, M., Turatsinze, J.V., Griebel, T., Villate, O., Santin, I., et al. (2014). RNA sequencing identifies dysregulation of the human pancreatic islet transcriptome by the saturated fatty acid palmitate. Diabetes *63*, 1978–1993. https://doi.org/10.2337/db13-1383.

9. Oh, Y.S., Bae, G.D., Baek, D.J., Park, E.Y., and Jun, H.S. (2018). Fatty acid-induced lipotoxicity in pancreatic beta-cells during development of type 2 diabetes. Front. Endocrinol. *9*, 384. https://doi.org/10.3389/fendo.2018.00384.

10. Šrámek, J., Němcová-fürstová, V., and Kovář, J. (2021). Molecular mechanisms of apoptosis induction and its regulation by fatty acids in pancreatic β-cells. Int. J. Mol. Sci. *22*, 4285. https://doi.org/10.3390/ijms22084285.

11. Small, J.C., Joblin-Mills, A., Carbone, K., Kost-Alimova, M., Ayukawa, K., Khodier, C., Dancik, V., Clemons, P.A., Munkacsi, A.B., and Wagner, B.K. (2022). Phenotypic Screening for Small Molecules that Protect β-Cells from Glucolipotoxicity. ACS Chem. Biol. *17*, 1131–1142. https://doi.org/10.1021/acschembio.2c00052.

12. Arner, P., and Kulyté, A. (2015). MicroRNA regulatory networks in human adipose tissue and obesity. Nat. Rev. Endocrinol. *11*, 276–288. https://doi.org/10.1038/nrendo.2015.25.

13. LaPierre, M.P., and Stoffel, M. (2017). MicroRNAs as stress regulators in pancreatic beta cells and diabetes. Mol. Metabol. *6*, 1010–1023. https://doi.org/10.1016/j.molmet.2017.06.020.

14. Han, Y.B., Wang, M.N., Li, Q., Guo, L., Yang, Y.M., Li, P.J., Wang, W., and Zhang, J.C. (2012). MicroRNA-34a contributes to the protective effects of glucagon-like peptide-1 against lipotoxicity in INS-1 cells. Chin. Med. J. (Taipei) *125*, 4202–4208. https://doi.org/10.3760/cma.j.issn.0366-6999.2012.23.008.

15. Lovis, P., Roggli, E., Laybutt, D.R., Gattesco, S., Yang, J.Y., Widmann, C., Abderrahmani, A., and Regazzi, R. (2008). Alterations in MicroRNA expression contribute to fatty Acid-Induced pancreatic β-Cell dysfunction. Diabetes *57*, 2728–2736. https://doi.org/10.2337/db07-1252.

16. Sims, E.K., Lakhter, A.J., Anderson-Baucum, E., Kono, T., Tong, X., and Evans-Molina, C. (2017). MicroRNA 21 targets BCL2 mRNA to increase apoptosis in rat and human beta cells. Diabetologia *60*, 1057–1065. https://doi.org/10.1007/s00125-017-4237-z.

17. Poy, M.N., Hausser, J., Trajkovski, M., Braun, M., Collins, S., Rorsman, P., Zavolan, M., and Stoffel, M. (2009). miR-375 maintains normal pancreatic α- and β-cell mass. Proc. Natl. Acad. Sci. USA *106*, 5813–5818. https://doi.org/10.1073/pnas.0810550106.

18. Lu, Y., Fei, X.-Q., Yang, S.-F., Xu, B.-K., and Li, Y.-Y. (2015). Glucose-induced microRNA-17 promotes pancreatic beta cell proliferation through down-regulation of Menin. Eur. Rev. Med. Pharmacol. Sci. *19*, 624–629.

19. Lu, H., Yang, J., Li, J., and Yuan, H. (2022). MiR-190 ameliorates glucotoxicity-induced dysfunction and apoptosis of pancreatic β-cells by inhibiting NOX2-mediated reactive oxygen species production. PeerJ *10*, e13849. https://doi.org/10.7717/peerj.13849.

20. Diener, C., Keller, A., and Meese, E. (2022). Emerging concepts of miRNA therapeutics: from cells to clinic. Trends Genet. *38*, 613–626. https://doi.org/10.1016/j.tig.2022.02.006.

21. Sandoval, D.A., and Patti, M.E. (2023). Glucose metabolism after bariatric surgery: implications for T2DM remission and hypoglycaemia. Nat. Rev. Endocrinol. *19*, 164–176. https://doi.org/10.1038/s41574-022-00757-5.

22. Langi, G., Szczerbinski, L., and Kretowski, A. (2019). Meta-analysis of differential miRNA expression after bariatric surgery. J. Clin. Med. *8*, 1220. https://doi.org/10.3390/jcm8081220.

23. Chick, W.L., Warren, S., Chute, R.N., Like, A.A., Lauris, V., and Kitchen, K.C. (1977). A transplantable insulinoma in the rat. Proc. Natl. Acad. Sci. USA *74*, 628–632. https://doi.org/10.1073/pnas.74.2.628.

24. Lavogina, D., Lust, H., Tahk, M.J., Laasfeld, T., Vellama, H., Nasirova, N., Vardja, M., Eskla, K.L., Salumets, A., Rinken, A., and Jaal, J. (2022). Revisiting the Resazurin-Based Sensing of Cellular Viability: Widening the Application Horizon. Biosensors *12*, 196. https://doi.org/10.3390/bios12040196.

25. Vichai, V., and Kirtikara, K. (2006). Sulforhodamine B colorimetric assay for cytotoxicity screening. Nat. Protoc. *1*, 1112–1116. https://doi.org/10.1038/nprot.2006.179.

26. Fernandes, H., Zonnari, A., Abreu, R., Aday, S., Barão, M., Albino, I., Lino, M., Branco, A., Seabra, C., Barata, T., et al. (2022). Extracellular vesicles enriched with an endothelial cell pro-survival microRNA affects skin tissue regeneration. Mol. Ther. Nucleic Acids *28*, 307–327. https://doi.org/10.1016/j.omtn.2022.03.018.

27. Caporarello, N., Parrino, C., Trischitta, V., and Frittitta, L. (2017). Insulin receptor signaling and glucagon-like peptide 1 effects on pancreatic beta cells. PLoS One *12*, e0181190. https://doi.org/10.1371/journal.pone.0181190.

28. Mishra, A., Liu, S., Promes, J., Harata, M., Sivitz, W., Fink, B., Bhardwaj, G., O'Neill, B.T., Kang, C., Sah, R., et al. (2021). Perilipin 2 downregulation in β cells impairs insulin secretion under nutritional stress and damages mitochondria. JCI Insight *6*, e144341. https://doi.org/10.1172/jci.insight.144341.

29. Lytrivi, M., Ghaddar, K., Lopes, M., Rosengren, V., Piron, A., Yi, X., Johansson, H., Lehtiö, J., Igoillo-Esteve, M., Cunha, D.A., et al. (2020). Combined transcriptome and proteome profiling of the pancreatic β-cell response to palmitate unveils key pathways of β-cell lipotoxicity. BMC Genom. *21*, 590. https://doi.org/10.1186/s12864-020-07003-0.

30. Marselli, L., Piron, A., Suleiman, M., Colli, M.L., Yi, X., Khamis, A., Carrat, G.R., Rutter, G.A., Bugliani, M., Giusti, L., et al. (2020). Persistent or Transient Human β Cell Dysfunction Induced by Metabolic Stress: Specific Signatures and Shared Gene Expression with Type 2 Diabetes. Cell Rep. *33*, 108466. https://doi.org/10.1016/j.celrep.2020.108466.

31. Taylor, H.J., Hung, Y.-H., Narisu, N., Erdos, M.R., Kanke, M., Yan, T., Grenko, C.M., Swift, A.J., Bonnycastle, L.L., Sethupathy, P., et al. (2023). Human pancreatic islet microRNAs implicated in diabetes and related traits by large-scale genetic analysis. Proc. Natl. Acad. Sci. USA *120*, e2206797120. https://doi.org/10.1073/pnas.2206797120.

32. Winter, T.J.J.D. (2025). Cell Type-specific eQTL Detection from Single-Cell RNA-Seq Reveals Post-transcriptional Regulatory Mechanisms in Human Islets, *1–48*.

33. Suleiman, M., Marselli, L., Cnop, M., Eizirik, D.L., De Luca, C., Femia, F.R., Tesi, M., Del Guerra, S., and Marchetti, P. (2022). The Role of Beta Cell Recovery in Type 2 Diabetes Remission. Int. J. Mol. Sci. *23*, 7435. https://doi.org/10.3390/ijms23137435.

34. Jiménez-Lucena, R., Rangel-Zúñiga, O.A., Alcalá-Díaz, J.F., López-Moreno, J., Roncero-Ramos, I., Molina-Abril, H., Yubero-Serrano, E.M., Caballero-Villarraso, J., Delgado-Lista, J., Castaño, J.P., et al. (2018). Circulating miRNAs as Predictive Biomarkers of Type 2 Diabetes Mellitus Development in Coronary Heart Disease Patients from the CORDIOPREV Study. Mol. Ther. Nucleic Acids *12*, 146–157. https://doi.org/10.1016/j.omtn.2018.05.002.

35. Kong, L., Zhu, J., Han, W., Jiang, X., Xu, M., Zhao, Y., Dong, Q., Pang, Z., Guan, Q., Gao, L., et al. (2011). Significance of serum microRNAs in pre-diabetes and newly diagnosed type 2 diabetes: A clinical study. Acta Diabetol. *48*, 61–69. https://doi.org/10.1007/s00592-010-0226-0.

36. Liu, R., Liu, C., He, X., Sun, P., Zhang, B., Yang, H., Shi, W., and Ruan, Q. (2022). MicroRNA-21 promotes pancreatic β cell function through modulating glucose uptake. Nat. Commun. *13*, 3545. https://doi.org/10.1038/s41467-022-31317-0.

37. Yerlikaya, F.H., and Öz, M. (2019). Aberrant expression of miRNA profiles in high-fat and high-sucrose fed rats. Clin. Nutr. Exp. *27*, 1–8. https://doi.org/10.1016/j.yclnex.2019.07.001.

38. Rong, Y., Bao, W., Shan, Z., Liu, J., Yu, X., Xia, S., Gao, H., Wang, X., Yao, P., Hu, F.B., and Liu, L. (2013). Increased microRNA-146a levels in plasma of patients with newly diagnosed type 2 diabetes mellitus. PLoS One *8*, e73272. https://doi.org/10.1371/journal.pone.0073272.

39. Yang, Z., Chen, H., Si, H., Li, X., Ding, X., Sheng, Q., Chen, P., and Zhang, H. (2014). Serum miR-23a, a potential biomarker for diagnosis of pre-diabetes and type 2 diabetes. Acta Diabetol. *51*, 823–831. https://doi.org/10.1007/s00592-014-0617-8.

40. Zaragosi, L.E., Wdziekonski, B., Brigand, K.L., Villageois, P., Mari, B., Waldmann, R., Dani, C., and Barbry, P. (2011). Small RNA sequencing reveals miR-642a-3p as a novel adipocyte-specific microRNA and miR-30 as a key regulator of human adipogenesis. Genome Biol. *12*, R64. https://doi.org/10.1186/gb-2011-12-7-r64.

41. Roomp, K., Kristinsson, H., Schvartz, D., Ubhayasekera, K., Sargsyan, E., Manukyan, L., Chowdhury, A., Manell, H., Satagopam, V., Groebe, K., et al. (2017). Combined lipidomic and proteomic analysis of isolated human islets exposed to palmitate reveals time-dependent changes in insulin secretion and lipid metabolism. PLoS One *12*, e0176391. https://doi.org/10.1371/journal.pone.0176391.

42. Somesh, B.P., Verma, M.K., Sadasivuni, M.K., Mammen-Oommen, A., Biswas, S., Shilpa, P.C., Reddy, A.K., Yateesh, A.N., Pallavi, P.M., Nethra, S., et al. (2013). Chronic glucolipotoxic conditions in pancreatic islets impair insulin secretion due to dysregulated calcium dynamics, glucose responsiveness and mitochondrial activity. BMC Cell Biol. *14*, 1–11. https://doi.org/10.1186/1471-2121-14-31.

43. Oliveira, A.F., Cunha, D.A., Ladriere, L., Igoillo-Esteve, M., Bugliani, M., Marchetti, P., Cnop, M., and A, O. (2015). In vitro use of free fatty acids bound to albumin: A comparison of protocols. Biotechniques *58*, 228–233. https://doi.org/10.2144/000114285.

44. Hauke, S., Keutler, K., Phapale, P., Yushchenko, D.A., and Schultz, C. (2018). Endogenous fatty acids are essential signaling factors of pancreatic B-cells and insulin secretion. Diabetes *67*, 1986–1998. https://doi.org/10.2337/db17-1215.

45. Hagman, D.K., Hays, L.B., Parazzoli, S.D., and Poitout, V. (2005). Palmitate inhibits insulin gene expression by altering PDX-1 nuclear localization and reducing MafA expression in isolated rat islets of Langerhans. J. Biol. Chem. *280*, 32413–32418. https://doi.org/10.1074/jbc.M506000200.

46. Sharma, R., Maity, S.K., Chakrabarti, P., Katika, M.R., Kapettu, S., Parsa, K.V.L., and Misra, P. (2023). PIMT Controls Insulin Synthesis and Secretion through PDX1. Int. J. Mol. Sci. *24*, 8084. https://doi.org/10.3390/ijms24098084.

47. Brom, M., Woliner-Van Der Weg, W., Joosten, L., Frielink, C., Bouckenooghe, T., Rijken, P., Andralojc, K., Göke, B.J., De Jong, M., Eizirik, D.L., et al. (2014). Non-invasive quantification of the beta cell mass by SPECT with 111In-labelled exendin. Diabetologia *57*, 950–959. https://doi.org/10.1007/s00125-014-3166-3.

48. Xu, G., Kaneto, H., Laybutt, D.R., Duvivier-Kali, V.F., Trivedi, N., Suzuma, K., King, G.L., Weir, G.C., and Bonner-Weir, S. (2007). Downregulation of GLP-1 and GIP receptor expression by hyperglycemia: Possible contribution to impaired incretin effects in diabetes. Diabetes *56*, 1551–1558. https://doi.org/10.2337/db06-1033.

49. Zhang, M., Bai, X., Du, Q., Xu, J., Wang, D., Chen, L., Dong, K., Chen, Z., and Yang, J. (2023). The Different Mechanisms of Lipid Accumulation in Hepatocytes Induced by Oleic Acid/Palmitic Acid and High-Fat Diet. Molecules *28*, 6714. https://doi.org/10.3390/molecules28186714.

50. El-Assaad, W., Buteau, J., Peyot, M.L., Nolan, C., Roduit, R., Hardy, S., Joly, E., Dbaibo, G., Rosenberg, L., and Prentki, M. (2003). Saturated fatty acids synergize with elevated glucose to cause pancreatic β-cell death. Endocrinology *144*, 4154–4163. https://doi.org/10.1210/en.2003-0410.

51. Listenberger, L.L., Han, X., Lewis, S.E., Cases, S., Farese, R.V., Ory, D.S., and Schaffer, J.E. (2003). Triglyceride accumulation protects against fatty acid-induced lipotoxicity. Proc. Natl. Acad. Sci. USA *100*, 3077–3082. https://doi.org/10.1073/pnas.0630588100.

52. Ryu, G.R., Yoo, J.M., Lee, E., Ko, S.H., Ahn, Y.B., and Song, K.H. (2011). Decreased expression and induced nucleocytoplasmic translocation of pancreatic and duodenal homeobox 1 in INS-1 cells exposed to high glucose and palmitate. Diabetes Metab. J *35*, 65–71. https://doi.org/10.4093/dmj.2011.35.1.65.

53. Garofalo, R.S., Orena, S.J., Rafidi, K., Torchia, A.J., Stock, J.L., Hildebrandt, A.L., Coskran, T., Black, S.C., Brees, D.J., Wicks, J.R., et al. (2003). Severe diabetes, age-dependent loss of adipose tissue, and mild growth deficiency in mice lacking Akt2/PKBβ. J. Clin. Investig. *112*, 197–208. https://doi.org/10.1172/JCI16885.

54. Kong, W., Peng, Y., Ji, C., Liu, Z., Gao, S., Zhang, Y., Chen, J., Li, X., Bao, M., Zhang, Y., et al. (2023). Akt2 deficiency alleviates oxidative stress in the heart and liver via up-regulating SIRT6 during high-fat diet-induced obesity. Clin. Sci. *137*, 823–841. https://doi.org/10.1042/CS20230433.

55. Liu, Y., Beyer, A., and Aebersold, R. (2016). On the Dependency of Cellular Protein Levels on mRNA Abundance. Cell *165*, 535–550. https://doi.org/10.1016/j.cell.2016.03.014.

56. Singh, V.P., Gurunathan, C., Singh, S., Singh, B., Lakshmi, B.J., Mishra, A.P., and Kumar, S. (2015). Genetic deletion of Wdr13 improves the metabolic phenotype of Lepr (db/db) mice by modulating AP1 and PPARγ target genes. Diabetologia *58*, 384–392. https://doi.org/10.1007/s00125-014-3438-y.

57. Hohoff, C., Zhang, M., Ambrée, O., Kravchenko, M., Buschert, J., Kerkenberg, N., Gorinski, N., Abdel Galil, D., Schettler, C., vom Werth, K.L., et al. (2019). Deficiency of the palmitoyl acyltransferase ZDHHC7 impacts brain and behavior of mice in a sex-specific manner. Brain Struct. Funct. *224*, 2213–2230. https://doi.org/10.1007/s00429-019-01898-6.

58. Cherian, P.T., Al-Khairi, I., Sriraman, D., Al-Enezi, A., Al-Sultan, D., AlOtaibi, M., Al-Enezi, S., Tuomilehto, J., Al-Mulla, F., Abubaker, J.A., and Abu-Farha, M. (2018). Increased circulation and adipose tissue levels of DNAJC27/RBJ in obesity and type 2-diabetes. Front. Endocrinol. *9*, 423. https://doi.org/10.3389/FENDO.2018.00423/PDF.

59. Rousseau, M., Denhez, B., Spino, C., Lizotte, F., Guay, A., Côté, A.-M., Burger, D., and Geraldes, P. (2022). Reduction of DUSP4 contributes to podocytes oxidative stress, insulin resistance and diabetic nephropathy. Biochem. Biophys. Res. Commun. *624*, 127–133. https://doi.org/10.1016/j.bbrc.2022.07.067.

60. Burr, M.L., Sparbier, C.E., Chan, Y.C., Williamson, J.C., Woods, K., Beavis, P.A., Lam, E.Y.N., Henderson, M.A., Bell, C.C., Stolzenburg, S., et al. (2017). CMTM6 maintains the expression of PD-L1 and regulates anti-Tumour immunity. Nature *549*, 101–105. https://doi.org/10.1038/nature23643.

61. Domschke, G., Linden, F., Pawig, L., Hafner, A., Akhavanpoor, M., Reymann, J., Doesch, A.O., Erbel, C., Weber, C., Katus, H.A., et al. (2018). Systematic RNA-interference in primary human monocyte-derived macrophages: A high-throughput platform to study foam cell formation. Sci. Rep. *8*, 10516. https://doi.org/10.1038/s41598-018-28790-3.

62. Preguiça, I., Alves, A., Nunes, S., Fernandes, R., Gomes, P., Viana, S.D., and Reis, F. (2020). Diet-induced rodent models of obesity-related metabolic disorders—A guide to a translational perspective. Obes. Rev. *21*, 1–29. https://doi.org/10.1111/obr.13081.

63. Alisi, A., Da Sacco, L., Bruscalupi, G., Piemonte, F., Panera, N., De Vito, R., Leoni, S., Bottazzo, G.F., Masotti, A., and Nobili, V. (2011). Mirnome analysis reveals novel molecular determinants in the pathogenesis of diet-induced nonalcoholic fatty liver disease. Lab. Invest. *91*, 283–293. https://doi.org/10.1038/labinvest.2010.166.

64. Bae, Y.U., Kim, Y., Lee, H., Kim, H., Jeon, J.S., Noh, H., Han, D.C., Ryu, S., and Kwon, S.H. (2019). Bariatric Surgery Alters microRNA Content of Circulating Exosomes in Patients with Obesity. Obesity *27*, 264–271. https://doi.org/10.1002/oby.22379.

65. Castaño, C., Meza-Ramos, A., Batlle, M., Guasch, E., Novials, A., and Párrizas, M. (2022). Treatment with EV-miRNAs Alleviates Obesity-Associated Metabolic Dysfunction in Mice. Int. J. Mol. Sci. *23*, 14920. https://doi.org/10.3390/ijms232314920.

66. Wiklander, O.P.B., Nordin, J.Z., O'Loughlin, A., Gustafsson, Y., Corso, G., Mäger, I., Vader, P., Lee, Y., Sork, H., Seow, Y., et al. (2015). Extracellular vesicle *in vivo* biodistribution is determined by cell source, route of administration and targeting. J. Extracell. Vesicles *4*, 26316. https://doi.org/10.3402/JEV.V4.26316.

67. Tsonkova, V.G., Sand, F.W., Wolf, X.A., Grunnet, L.G., Kirstine Ringgaard, A., Ingvorsen, C., Winkel, L., Kalisz, M., Dalgaard, K., Bruun, C., et al. (2018). The EndoC-βH1 cell line is a valid model of human beta cells and applicable for screenings to identify novel drug target candidates. Mol. Metabol. *8*, 144–157. https://doi.org/10.1016/j.molmet.2017.12.007.

68. Amorim, R., Simões, I.C.M., Veloso, C., Carvalho, A., Simões, R.F., Pereira, F.B., Thiel, T., Normann, A., Morais, C., Jurado, A.S., et al. (2021). Exploratory data analysis of cell and mitochondrial high-fat, high-sugar toxicity on human hepg2 cells. Nutrients *13*, 1723. https://doi.org/10.3390/nu13051723.

69. Acosta-Montalvo, A., Saponaro, C., Kerr-Conte, J., Prehn, J.H.M., Pattou, F., and Bonner, C. (2020). Proglucagon-Derived Peptides Expression and Secretion in Rat Insulinoma INS-1 Cells. Front. Cell Dev. Biol. *8*, 590763. https://doi.org/10.3389/fcell.2020.590763.

70. Nibbelink, M.G., Marchioli, G., Moroni, L., Karperien, M., and Van Apeldoorn, A. (2016). A protocol to enhance INS1E and MIN6 functionality—The use of theophylline. Int. J. Mol. Sci. *17*, 1–9. https://doi.org/10.3390/ijms17091532.

71. Livak, K.J., and Schmittgen, T.D. (2001). Analysis of relative gene expression data using real-time quantitative PCR and the 2-ΔΔCT method. Methods *25*, 402–408. https://doi.org/10.1006/meth.2001.1262.

72. Cock, P.J.A., Fields, C.J., Goto, N., Heuer, M.L., and Rice, P.M. (2010). The Sanger FASTQ file format for sequences with quality scores, and the Solexa/Illumina FASTQ variants. Nucleic Acids Res. *38*, 1767–1771. https://doi.org/10.1093/nar/gkp1137.

73. Kim, D., Langmead, B., and Salzberg, S.L. (2015). HISAT: A fast spliced aligner with low memory requirements. Nat. Methods *12*, 357–360. https://doi.org/10.1038/nmeth.3317.

74. Kozomara, A., Birgaoanu, M., and Griffiths-Jones, S. (2019). MiRBase: From microRNA sequences to function. Nucleic Acids Res. *47*, D155–D162. https://doi.org/10.1093/nar/gky1141.

75. Enright, A.J., John, B., Gaul, U., Tuschl, T., Sander, C., and Marks, D.S. (2003). Enright-2003-Genomebiol.Pdf. Genome Biol. *5*, R1.

76. Nunes, S., Alves, A., Preguiça, I., Barbosa, A., Vieira, P., Mendes, F., Martins, D., Viana, S.D., and Reis, F. (2020). Crescent-like lesions as an early signature of nephropathy in a rat model of prediabetes induced by a hypercaloric diet. Nutrients *12*, 881. https://doi.org/10.3390/nu12040881.

77. Zhao, F., Cheng, L., Shao, Q., Chen, Z., Lv, X., Li, J., He, L., Sun, Y., Ji, Q., Lu, P., et al. (2020). Characterization of serum small extracellular vesicles and their small RNA contents across humans, rats, and mice. Sci. Rep. *10*, 4197. https://doi.org/10.1038/s41598-020-61098-9.

78. Gardiner, C., Ferreira, Y.J., Dragovic, R.A., Redman, C.W.G., and Sargent, I.L. (2013). Extracellular vesicle sizing and enumeration by nanoparticle tracking analysis. J. Extracell. Vesicles *2*, 1–11. https://doi.org/10.3402/jev.v2i0.19671.

79. Smith, P.K., Krohn, R.I., Hermanson, G.T., Mallia, A.K., Gartner, F.H., Provenzano, M.D., Fujimoto, E.K., Goeke, N.M., Olson, B.J., and Klenk, D.C. (1985). Measurement of protein using bicinchoninic acid. Anal. Biochem. *150*, 76–85. https://doi.org/10.1016/0003-2697(85)90442-7.